I. K. Karoussis
N. P. Lang

PERI-IMPLANTITIS

From Diagnosis to Treatment

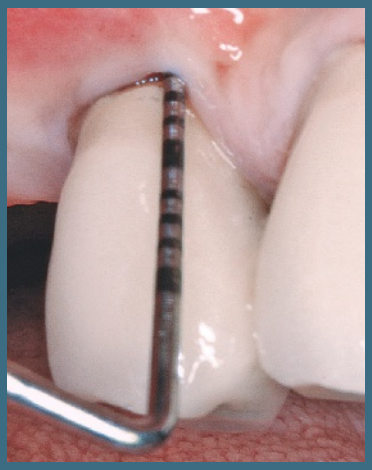

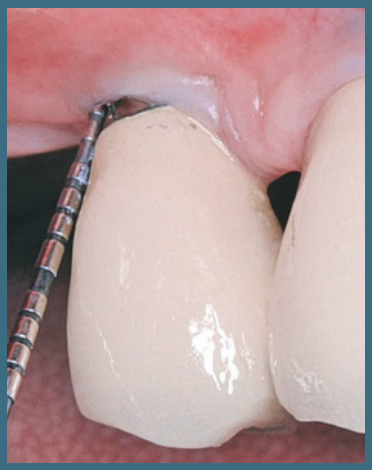
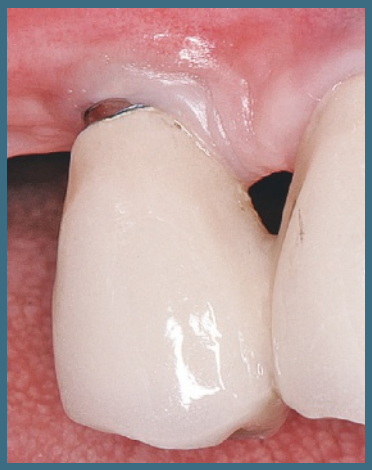

In collaboration with P. Ntokou

QUINTESSENCE PUBLISHING

I. K. Karoussis
N. P. Lang

PERI-IMPLANTITIS

From Diagnosis to Treatment

In collaboration with P. Ntokou

QUINTESSENCE PUBLISHING

Berlin | Chicago | Tokyo
Barcelona | London | Milan | Mexico City | Paris | Prague | Seoul | Warsaw
Beijing | Istanbul | Sao Paulo | Zagreb

One book, one tree: In support of reforestation worldwide and to address the climate crisis, for every book sold Quintessence Publishing will plant a tree (https://onetreeplanted.org/).

A CIP record for this book is available from the British Library.

QUINTESSENCE PUBLISHING DEUTSCHLAND

Quintessenz Verlags-GmbH
Ifenpfad 2–4
12107 Berlin, Germany
www.quintessence-publishing.com

Quintessence Publishing Co Ltd
Grafton Road, New Malden
Surrey KT3 3AB, United Kingdom
www.quintessence-publishing.com

Editing and reproduction: Quintessenz Verlags-GmbH, Berlin, Germany
Layout and production: Janina Kuhn, Quintessenz Verlags-GmbH, Berlin, Germany

ISBN 978-1-78698-145-5
Printed and bound in Croatia

Foreword

This book provides a comprehensive overview of the key aspects of diagnosis and treatment of peri-implantitis. The illustrative chapters include many case examples describing situations readers may encounter in their everyday practice, providing practical insights into the management of these complications. The chapters address a range of treatment approaches from non-surgical to surgical management, resective and regenerative treatment, and procedures for peri-implant soft tissue augmentation.

Both authors are renowned for their extensive experience in the fields of implant dentistry, periodontology, and management of peri-implantitis, with Professor Lang having developed the first comprehensive treatment protocol for peri-implantitis known as Cumulative Interceptive Supportive Therapy (CIST), which forms the basis for the contemporary treatment approaches outlined in the book.

The comprehensive approach includes chapters covering the etiology, diagnosis, prevalence, and risk factors for peri-implantitis as well as decision-making steps for treatment planning and practical steps for treatment. The book concludes with key steps for prevention and supportive peri-implant treatment. This informative and illustrative book provides a practical and useful guide for all oral health professionals who practice in the field of implant dentistry.

Lisa J. A. Heitz-Mayfield
Perth, Western Australia, August 2024
Editor-in-Chief
Clinical Oral Implants Research

To our families, with love
and gratitude

Introduction

Peri-implantitis: from diagnosis to treatment is a monograph that aims to present, in a structured and detailed manner, the sum of all available information regarding peri-implant tissue pathology, as well as the knowledge and "secrets" clinicians should be aware so that they can successfully approach the treatment of peri-implant diseases. The tremendously high number of implants placed in millions of patients globally makes knowledge of the treatment of pathologic situations that concern them necessary. In the past, peri-implant diseases were a subject of study for many clinicians and researchers to clarify the etiology and factors that predispose to peri-implantitis or worsen its progress, as well as ways to treat it.

Now that the use of implants has been established in daily clinical practice, it is clear that on occasions, once the highly anticipated osseointegration has been achieved, soft tissue inflammation and gradual bone loss around the implants, which were already functional, may occur at different times. These initial observations caused scientific debate, with some researchers even disputing the existence of peri-implantitis. Later on, many scientists regarded peri-implantitis as a problem that only affected rough implants or implants placed transmucosally. However, since the early 1990s, many researchers have investigated the issue carefully and recognized and named the diseases that affect peri-implant tissues, thus initiating a growing and ongoing interest in and knowledge of the factors that contribute to the establishment and progress of peri-implant diseases, while also seeking more effective therapies. Unfortunately, it soon became clear that treating implants as if they were teeth and treating peri-implant diseases using the same therapies used for periodontal diseases did not achieve satisfactory results.

Even though studies, conferences, and scientific research have reported on specific issues that concern peri-implantitis, there is a significant lack of concentrated knowledge and information about the subject presented through the pages of a book; at a global level, very few published efforts have solely focused on this subject. Thus, to this day, many clinicians apply what they believe is correct, often using tools and techniques that are not adequately documented. This is understandable to a certain extent because clinical application precedes statistical evaluation through research. Moreover, it is not uncommon for some of the interventions used to cause more problems than the ones they are aiming to solve.

Diagnosis and treatment of peri-implantitis are very demanding. This book is a natural by-product of the engagement with implantology through the prism and philosophy of periodontology, but also of the need to gather and assess existing knowledge. The continuous stream of information available via the international literature has been combined with the clinical experience acquired from our courses run at the Periodontology Clinics of the Universities of Athens and Bern, but mainly from treating many patients with peri-implantitis; these have been entrusted to us by many colleagues and patients to whom we owe our warm thanks.

This book is mainly aimed at dental practitioners involved in implantology, either through general dentistry or as a clinical specialization, as well as dental students who want to deepen their knowledge of how to prevent, diagnose, and treat peri-implantitis. Relevant information is provided in a detailed form, guided by necessary and available scientific documentation, offering conclusions gained from the critical evaluation of scientific research. The text is accompanied by a plethora of images that complement, support, and help to interpret scientific knowledge, while also offering a step-by-step methodology; they also complement the techniques presented, depending on the specific indications for each technique. Some of the images have been provided by colleagues or the Departments of Periodontology of the Dental Schools in Athens and Bern.

Schematic illustration, where necessary, helps the reader to understand the pathologic indications for and the application of certain techniques, which are presented in detail via carefully chosen images.

We express our respect and thanks to all those who have played an important role in the creation of this book. We offer our never-ending gratitude to our families and all our teachers, without exception, for their love and support.

Our most heartfelt thanks go to our colleague Dr Panagiota Ntokou; her contribution to the writing of several of the chapters was not only valuable but also plentiful, and her collaboration is rightfully recognized and honored on the book's cover.

We offer warm thanks to Dr Spyridon Silvestros, Assistant Professor at the National and Kapodistrian University of Athens (NKUA), for his collaboration in the writing of Chapter 12.

For the exceptional quality of the illustrations and sketches, we thank Mrs Zoe Karoussi-Patsilinakou.

We thank Dr Kyriaki Kyriakidou for her scientific collaboration and for photographing many laboratory essays used in the book.

We also thank Drs Leonidas Podaropoulos and Paolo Trisi, and Associate Professor Demos Kalyvas, for allowing us to reproduce the histologic images in Fig 1-5a, b, 1-6, 2-1, 2-12, 2-22, and 7-2; Dr Ioannis Fandrides and Professor Triantafyllos Papadopoulos for Fig 1-7a, b, 1-8, 1-9a, b, 1-10a, b, 1-11, 1-12a, b, 2-14a, b, 2-15, 2-17a, b, 2-18, 2-19a, b, and 2-20; and Dr Eustathia Tsetsenekou for allowing us to reproduce the histologic images in Fig 2-7, 2-10a, b, and 2-11a–d.

We thank Dr George Vilos, Oral and Maxillofacial Surgeon, for allowing us to reproduce the images in Fig 6-6, 9-14a–d, 9-16a–e, and 15-8a–f; Dr Nikolaos Nikitakis, Professor of Oral Medicine, for Fig 9-15; Dr Demitrios Vlahodimitropoulos, Associate Professor of Medicine, for Fig 9-17; the Department of Periodontology at NKUA for Fig 9-25a, b, 9-26a–f, and 13-11a–f; and Dr Andreas Gkogkos for Fig 13-11g, h.

We want this book to be a source of information and clinical guidance with regard to the approach dental practitioners must learn and apply to better treat patients who already have or are due to receive implants to rehabilitate complete or partial edentulism.

Ioannis K. Karoussis
Professor of Periodontology

Niklaus P. Lang
Professor of Periodontology

Authors

Prof Ioannis K. Karoussis, DDS, MS, Dr med dent

Professor Ioannis K. Karoussis graduated from the Dental School of Athens, Greece, where he also achieved his Master's degree in Oral Biology. He specialized in Periodontology and Implantology at the Universities of Athens, Greece and Bern, Switzerland, where he also completed his doctoral thesis. He has served as coordinator of the Postgraduate clinic of Periodontology at the University of Athens, as Editor of the Journal "Odontostomatological Progress" and President of the Hellenic Society for Odontostomatological Research. His private practice in Athens specializes in periodontics and implant dentistry. He has received awards for his research on peri-implantitis and has authored more than 100 papers in peer-reviewed journals as well as four textbooks in the Greek language.

Prof em Niklaus P. Lang, DMD, MS, PhD, Dr odont hc

Professor Niklaus P. Lang is the author of more than 730 publications. He holds four honorary doctorates and honorary membership of 20 national and international associations. In 1968, he was awarded the Swiss Dental Association's renowned Prix Louis Metzger, and in 1992, he received the IADR's Basic Science in Periodontal Disease Award. He is a past president of the ITI and the Swiss Society for Periodontology (SSP) and was Editor-in-Chief of the journal "Clinical Oral Implants Research" until 2016. He is active in clinical research related to implant dentistry, periodontology, etiology and pathogenesis of peri-implant infections, risk evaluation, wound healing, and oral microbiology. From 2008 to 2012, he built up the curriculum in implant dentistry at the University of Hong Kong after having headed the Department of Periodontology and Fixed Prosthodontics at the University of Bern, Switzerland from 1978 to 2008.

Contents

1 Anatomy of Periodontal and Peri-Implant Tissues

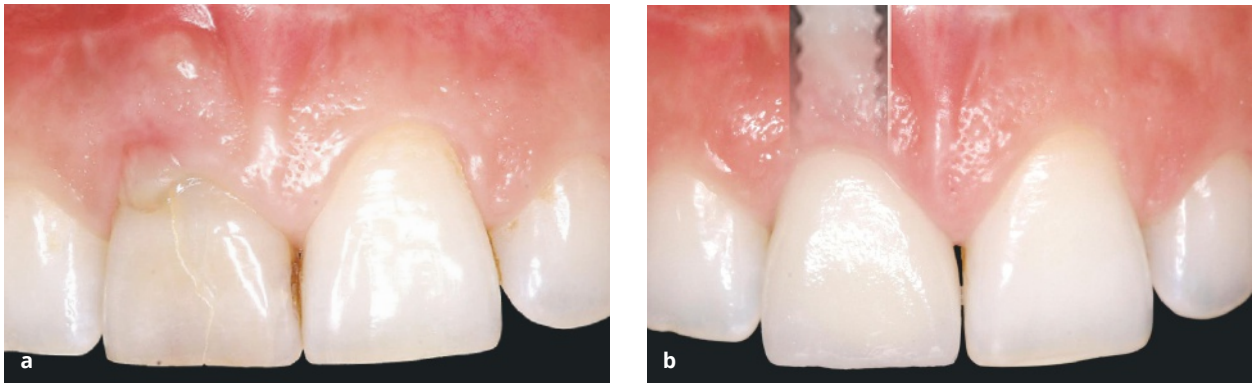

Figs 1-1a, b **(a)** Tooth 11 with a vertical root fracture, warranting its extraction. **(b)** An implant has been placed to replace tooth 11. The peri-implant mucosa shows no esthetic or functional differences compared to the gingiva of the adjacent teeth.

The clinical and histologic imaging of the tissues surrounding teeth and implants present many similarities but also some differences. To better understand the pathology of tissues, the prerequisite is an in-depth knowledge of and familiarization of the clinician with the physiology and anatomy of periodontal and peri-implant tissues.

Periodontal tissues consist of the gingiva, the periodontal membrane, the root cementum, and the alveolar bone. If a tooth is lost, the term "gingiva" is no longer used as an anatomic term and is replaced by the term "peri-implant mucosa". Thus, peri-implant tissues consist of the peri-implant mucosa and the alveolar bone.

The gingiva surround the neck of the tooth and constitute the coronal portion of the oral mucosa. The peri-implant mucosa is the continuation of the oral mucosa toward the crest of the alveolar ridge and surrounds the neck of the implants. The gingiva and peri-implant mucosa have many functional, anatomic, and immunologic similarities. In a healthy mouth, both the gingiva and the peri-implant mucosa are usually a light pink color and are covered with a keratinized epithelium externally (Figs 1-1a, b).[1,2]

The gingiva serve as a barrier against microbes, thus protecting the underlying tissue, and also play a significant role in sensation, phonetics, and esthetics. Both structures constitute the limit between the external environment and the internal organism. Whether a submerged, transmucosal, or non-submerged healing protocol is applied, soft tissue adhesion and protection of osseointegration function in the same way.

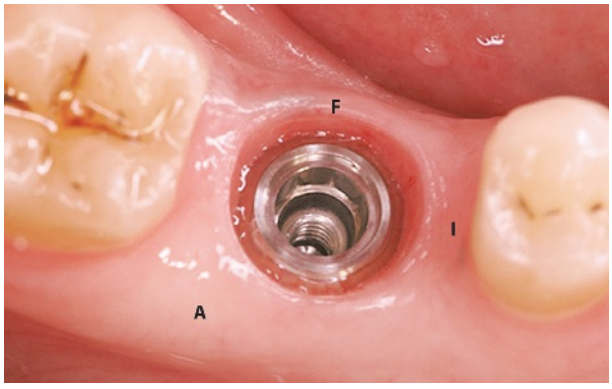

Fig 1-2 The peri-implant mucosa: free **(F)**, attached **(A)**, and interdental **(I)**.

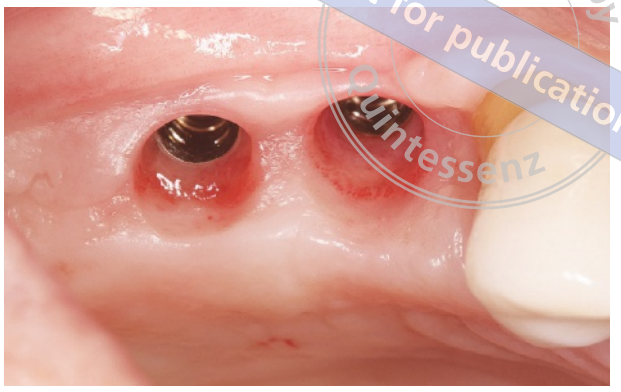

Fig 1-3 Clinical image after the removal of the provisional implant prosthesis. Note the healthy appearance of the peri-implant tissues, despite the deep peri-implant sulcus due to the increased thickness of the peri-implant mucosa. This may be attributed to the bone loss that occurred because of previous chronic periodontitis.

1.1 Anatomy

The gingiva and peri-implant mucosa extend from the mucogingival junction to the soft tissue margin. Depending on their topographic positioning, they may be distinguished into:

- free gingiva and free peri-implant mucosa;
- attached gingiva and attached peri-implant mucosa;
- interdental papilla and interdental peri-implant mucosa (Fig 1-2).

The free gingiva surrounds teeth without being attached to them, hence it constitutes the histologic sulcus. The same applies to the free peri-implant mucosa. The free gingiva morphologically follows the necks of the teeth; in a healthy mouth, it has a scalloped course that follows the outline of the cementoenamel junction. In the case of implants, however, the free peri-implant mucosa does not follow a scalloped course. Formation of an interdental papilla between two adjacent implants depends on several factors that may include the height of the alveolar bone on the buccal site and, in the area between implants, the distance between the contact point of the implant crown and the adjacent teeth or implants.

In a healthy mouth, the free gingiva has a smooth surface and a width of 1 to 2 mm. The space between the tooth and free gingival surface is known as the gingival crevice. The same space between the free peri-implant mucosa and the implant surface is referred to as the peri-implant crevice. The gingival crevice can be up to 3 mm deep in a healthy mouth, whereas the peri-implant sulcus can be up to 4 mm deep. A gingival crevice with a depth greater than 3 mm may represent a pathologic deepening of the gingival sulcus, which is due to the apical, pathologic migration of the junctional epithelium. In peri-implant tissues, the peri-implant sulcus can be deeper than 4 mm. This happens in cases where the implant was initially placed in a more apical position for esthetic reasons.

Determining a pathologic condition at implant sites involves recording the thickness of the mucosa at the time of placement and measuring the depth of the peri-implant sulcus. It also involves keeping detailed records of radiographs. Consequently, it is possible to precisely estimate any pathologic changes in the attachment of the peri-implant tissues and the height of the peri-implant bone (Fig 1-3).[3] More details on this issue can be found in Chapter 7.

1.2 Junctional epithelium

The junctional epithelium around the teeth has a mean width of 1 to 2 mm; for implants, the width is approximately 2 to 3 mm.[4] The junctional epithelium may adhere to materials like titanium or ceramics via a basal membrane and hemidesmosomes, as also observed in teeth. The thickness of the junctional epithelium varies between 30 and 100 µm. Its coronal

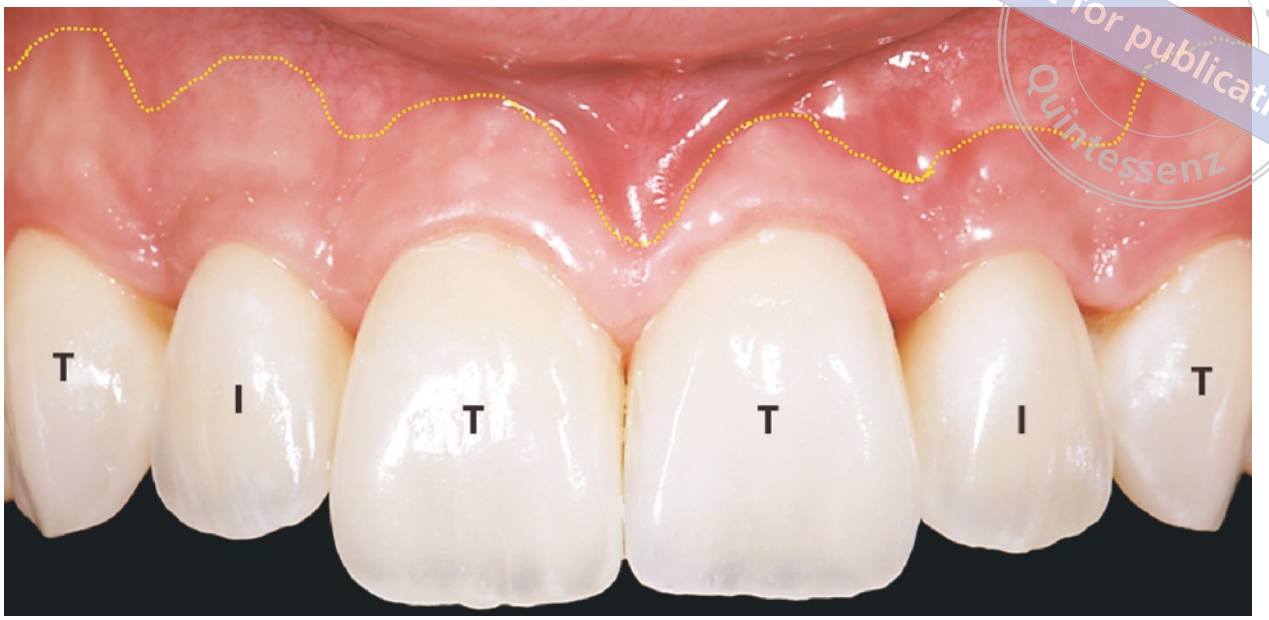

Fig 1-4 Clinical image after the completion of the implant crowns in sites 12 and 22, and ceramic veneers in sites.11, 13, 21, and 23. The health of the peri-implant tissues can be seen, as well as the resemblance between periodontal and peri-implant tissues once clinically examined. T, tooth; I, implant. The dotted yellow line represents the mucogingival junction.

end contains one to thirty cell layers; at its apical end, it is narrower and contains about three to four layers. The junctional epithelium of teeth and implants lacks keratinization. Junctions between cells are achieved by adhesion molecules; that is, receptors on the cell surface, mainly integrins and cadherins.[5]

The similarities between the junctional epithelium of teeth and implants provide the functional characteristics for adhesion (such as intercellular adhesion molecule 1 [ICAM-1]).[6] In histologic imaging, migration of leukocytes through the pericellular spaces is observed. Moreover, production of tissue-type plasminogen activator may be noted exactly where the junctional epithelium of the gingiva or the peri-implant epithelium change to the junctional epithelium[7].

In addition, the pericellular spaces in the junctional epithelium are wider compared to other types of epithelium. This may explain the increased permeability of the junctional epithelium to antigenic stimuli and inflammatory cells. The junctional epithelium is also characterized by rapid cell turnover, thereby providing a defense mechanism for healing. It also plays a crucial role in the healing process as it represents a rapid rate of cell renewal.[8] This extremely fast renewal of the junctional epithelium contributes to the defense and protection of the bottom parts of the gingival and peri-implant crevices against microbial challenges.[9,10]

At the apical end of the free gingiva or peri-implant mucosa is the attached gingiva or mucosa. For the gingiva, in a healthy mouth, a groove may be observed, known as the free gingival groove. This groove is not always distinguishable and it is usually absent around implants. The line of free gingiva corresponds to the coronal part of the supracrestal connective tissue fibers, which insert into the root cementum as Sharpey fibers.

These attached tissues extend apically to the border of the nonkeratinized lining of the oral mucosa. The distinguishable line in the transition zone is the mucogingival junction in natural teeth, while the same term is erroneously used for implants (Fig 1-4). A zone consisting of connective tissue fibers can also be observed on peri-implant tissues, between the apical border of the junctional epithelium and the alveolar bone crest. This zone is approximately 1 to 2 mm long. After placement of a non-submerged implant, the titanium oxide layer that covers the implant surface interacts with the deeper layer of connective tissue that covers the alveolar ridge; this stops the apical migration of the epithelium, showing that the organism does not recognize this area as a foreign body. The phenomenon is called"'connective tissue adaptation" (Figs 1-5a, b).

The connective tissue around implants is rich in collagen fibers, as observed under light and elec-

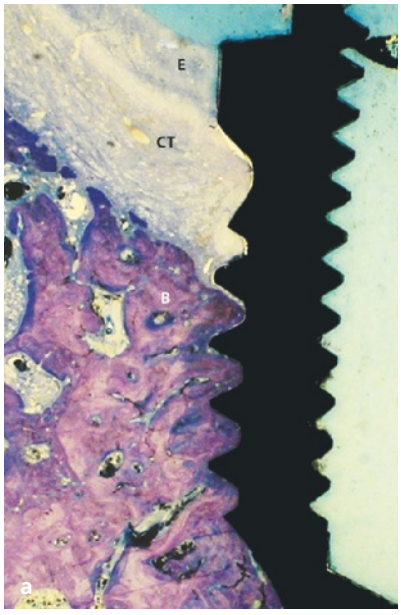

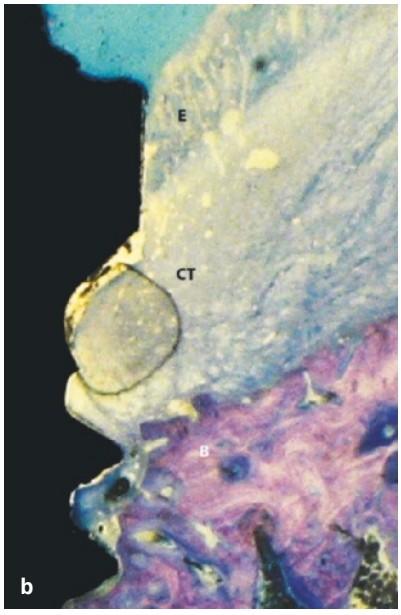

Figs 1-5a, b Histologic images derived from an animal (dog), where the peri-implant tissues are shown. B, bone; CT, connective tissue; E, epithelium. The circular formation shown in **(b)** is an artifact. Apart from the bone, peri-implant soft tissues seem to adhere to the implant, creating a natural barrier against bacterial invasion. The epithelium and implant surface or the surface of the implant restoration separate the peri-implant crevice (courtesy of Drs L. Podaropoulos, P. Trisi, and D. Kalyvas).

Fig 1-6 Histologic sample derived from an animal (dog), where a titanium implant and its interaction with the adjacent peri-implant tissues can be observed, long after its placement. B, bone; CT, connective tissue; I, implant. The yellow arrow indicates the direct contact of the connective tissue with the implant surface (courtesy of Drs L. Podaropoulos, P. Trisi, and D. Kalyvas).

tron microscopy. However, the supracrestal fibers beneath the junctional epithelium may not have the same orientation in natural teeth.

1.3 Connective tissues

The connective tissues of the gingiva and peri-implant mucosa are the largest part of the soft tissues (attached, free, and interdental) and occupy the space between the epithelium and the alveolar ridge (Fig 1-6). They consist of collagen (60%), oxytalan, reticular and elastic fibers, as well as fibroblasts (5%), the extracellular matrix, blood vessels (35%), and nerves. Connective tissue adjoins the epithelium via the intervention of the basal membrane.

Types I and III collagen fibers, known as gingival fibers, are arranged in a dense mesh and are distinguished according to their primary (dentogingival, alveolo-gingival, dentoperiosteal, circular, transeptal) and secondary orientation (interdental papillary, transgingival, semicircular).

Experimental studies have shown that connective tissue fibers are arranged laminarly to the implant surface. It has been suggested that the orientation of peri-implant connective tissue collagen fibers depends on the existence of keratinized mucosa and the surface roughness of the implant. When the zone of keratinized attached peri-implant mucosa is inadequate, connective tissue fibers are parallel to the implant surface, whereas fibers have a more vertically oriented direction to the implant when there is an abundance of attached keratinized mucosa. Moreover, when adjacent to a rough surface, collagen fibers may present a functional orientation. Scanning electron microscopy of the mesophase between connective tissue and non-submerged implants suggests that some connective tissue fibers are vertically oriented toward the implant surface. Moreover, they come into contact with a glycosaminoglycan layer that covers the implant surface.[11] In addition, rough implant surfaces promote the adhesion of epithelial cells and fibroblasts. However, they also favor the accumulation of microorganisms (Figs 1-7a, b to 1-12a, b).[12,13]

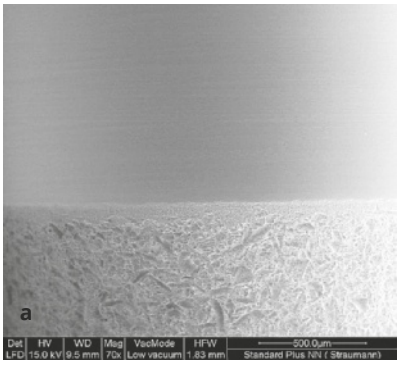

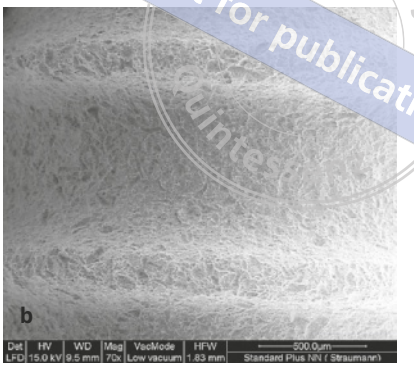

Figs 1-7a, b Micrographs (×70). **(a)** A Straumann implant; specifically, its smooth transmucosal part and its rough part, which must be covered with bone, are shown. **(b)** Part of the rough surface showing two threads and the space between them. The surface was sandblasted with 250- to 500-µm Al_2O_3 grains and acid-etched with HCl + H_2SO_4 at 130°C for 5 minutes (courtesy of Drs T. Papadopoulos and I. Fandridis).

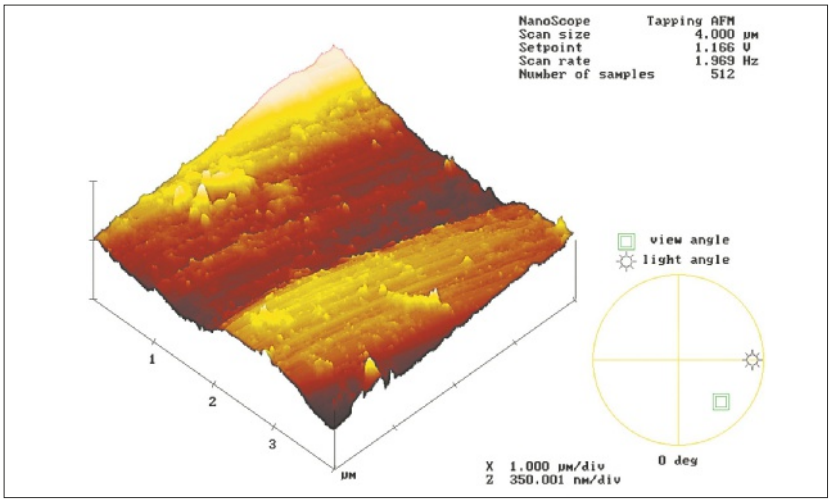

Fig 1-8 Atomic force microscopy reveals the very low roughness of the smooth Straumann surface, which promotes the adhesion of epithelial cells through hemidesmosomes (courtesy of Drs T. Papadopoulos and I. Fandridis).

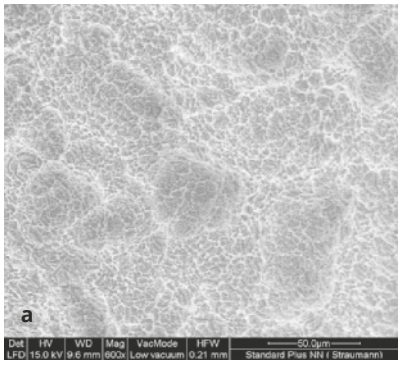

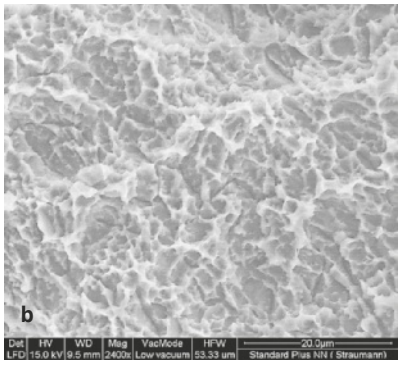

Figs 1-9a, b Scanning electron micrographs. **(a)** The rough surface of the Straumann implant is presented at ×600 magnification. **(b)** The same surface is presented at ×2,400 magnification. The rough surface promotes adhesion and the proliferation of osteoblasts (courtesy of Drs T. Papadopoulos and I. Fandridis).

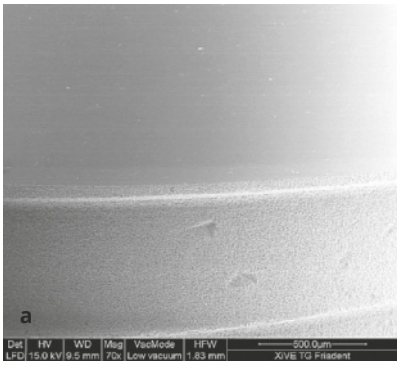

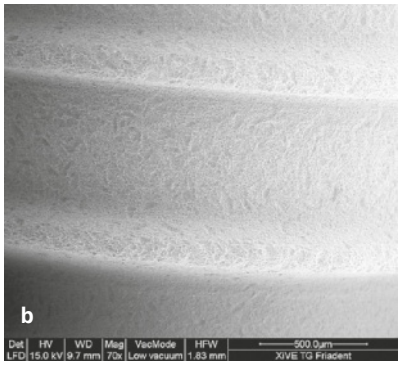

Figs 1-10a, b Scanning electron micrographs (×70). The Xive implant (Dentsply Sirona, Charlotte, NC, USA) is shown. **(a)** The smooth part of the implant, and its rough part that must be placed in the bone, can be seen. **(b)** Part of the surface containing two threads and the space in between them can be observed. The rough surface was airborne-particle abraded with Al_2O_3 grains and chemically acid-etched (courtesy of Drs T. Papadopoulos and I. Fandridis).

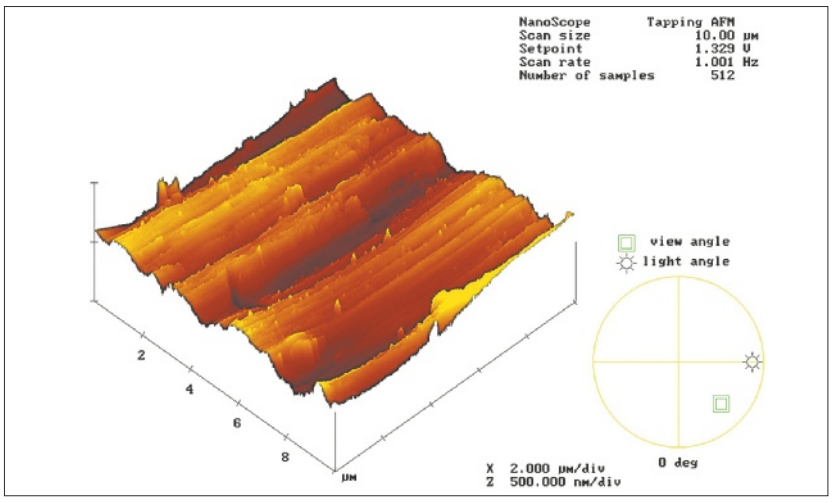

Fig 1-11 Atomic force microscopy revealed the low roughness of the smooth surface of the Xive implant, which promotes the adhesion of epithelial cells through hemidesmosomes (courtesy of Drs T. Papadopoulos and I. Fandridis).

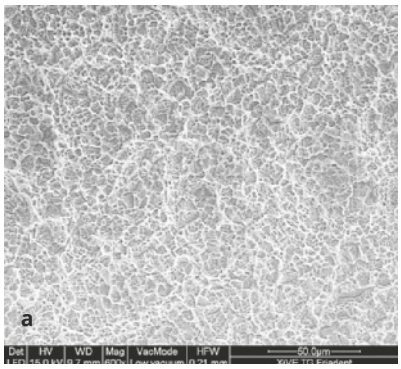

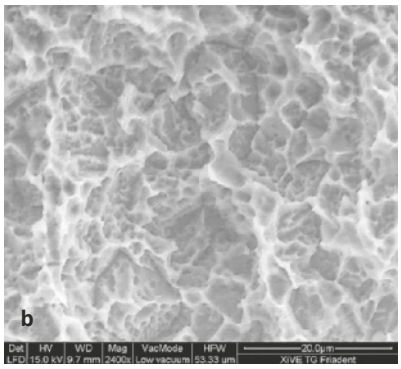

Figs 1-12a, b Scanning electron micrographs. **(a)** The rough surface of the Xive implant is presented at ×600 magnification. **(b)** The same surface is presented at ×2,400 magnification. The rough surface promoted the proliferation and maturation of osteoblasts (courtesy of Drs T. Papadopoulos and I. Fandridis).

Connective tissue around implants has two zones: an internal and an external zone. The internal zone has a thickness of 50 to 100µm thickness and 67% of its mass consists of collagen fibers and 32% consists of fibroblasts, while blood vessels are essentially absent (0.3%), thus resembling scar tissue.

In the external zone, which is 60 µm thick, more collagen fibers and fewer fibroblasts may be observed (85% and 11%, respectively, compared to 3% for vascular structures).

Apart from fibroblasts, the connective tissues of the gingiva and peri-implant mucosa contain inflammatory cells (multinuclear cells, lymphocytes, macrophages, mast cells, and basophilic and eosinophilic granulocytes).

Because they constitute about 65% of connective tissue cells and are arranged between fibers, that is, they are parallel to collagen fibers, fibroblasts are the most abundant group of cells (Figs 1-13 to 1-15).[14,15]

Nevertheless, the connective tissue of the peri-implant mucosa has fewer cellular elements and more collagen compared to the connective tissue around teeth. Immunohistochemical methods showed fundamental differences between healthy peri-implant and periodontal tissues. Types V and VI collagen are distributed differently, while types I, III, IV, and VII, as well as fibronectin, have similar distributions.[16]

1.4 Vascularization

Gingival connective tissue shows rich vascularization, which is mediated by the blood vessels of the periodontal membrane, the blood vessels of the oral mucosa, and vessels that extend through the periosteum. These vessels form an afferent arterial and efferent venous network, which are interlaced in two rich vascular meshes, one below the oral and junctional epithelium and one below the attached epithelium, known as the hypoepithelial vascular mesh. Specialized cells expressing adhesive molecules (such as endothelial-leukocyte adhesion molecule 1 [ELAM-1] and ICAM-1) facilitate the transport of leukocytes.[17]

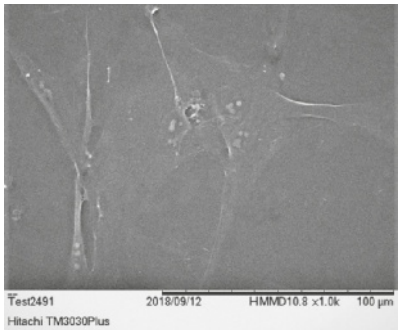

Fig 1-13 Micrograph (×1,000) of human gingival fibroblasts cultured for 24 hours on β-tricalcium phosphate surfaces.

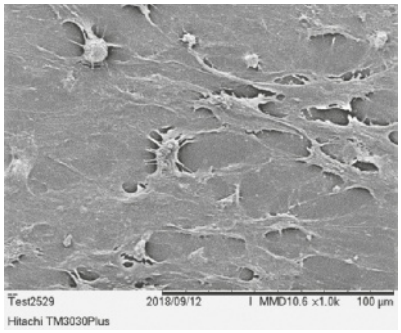

Fig 1-14 Micrograph (×1,000) of human gingival fibroblasts cultured for 72 hours on β-tricalcium phosphate surfaces, after irradiation with an 810-nm diode laser.

Fig 1-15 Fluorescence microscopy image (×20) of human gingival fibroblasts cultured on β-tricalcium phosphate surfaces for 24 hours. Their characteristic elongated morphology can be seen.

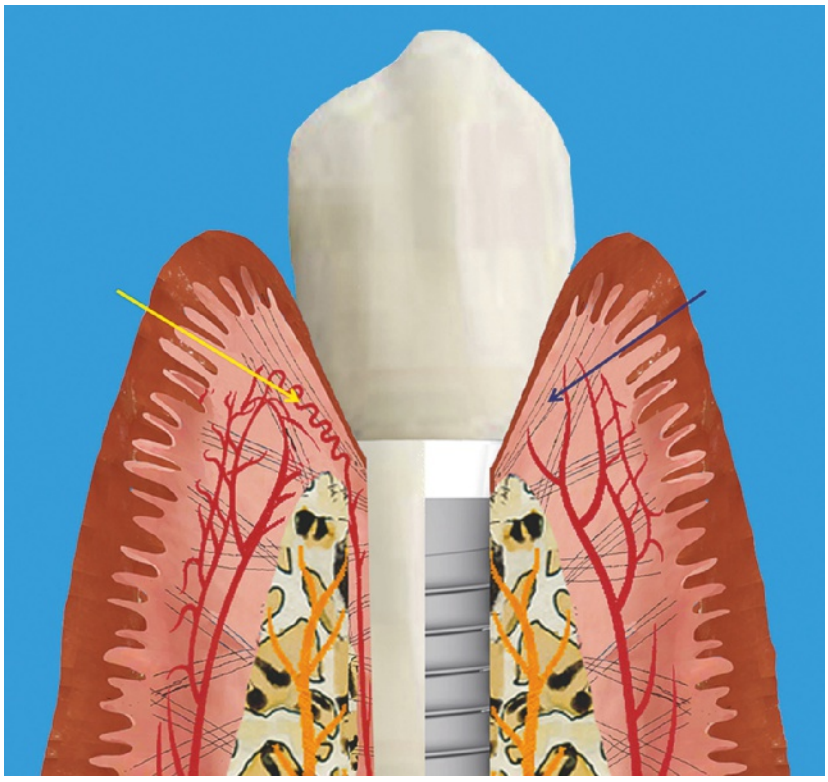

Fig 1-16 Schematic illustration of periodontal and peri-implant tissues demonstrating vascularization.

In peri-implant tissues, there is no periodontal membrane; hence, vascularization originating from it is absent. Thus, the peri-implant mucosa is solely supplied by vessels that emerge from the periosteum. As a result, the tissue below the attached epithelium of implants has reduced vascularization. The lack of a collateral circulation reduces the response of the peri-implant mucosa to inflammation and predisposes to faster peri-implant bone destruction (Fig 1-16).[18]

At implants, both subepithelial vascular mesh and periodontal membrane are missing as the titanium surface is in direct structural and functional contact with the surrounding bone. Moreover, Sharpey fibers that usually insert into the root cementum are absent, and supracrestal connective tissue fibers course parallel to the implant surface.

Lymphatic drainage of the gingiva and peri-implant mucosa is similar, although lymphatic capillaries are missing in the latter. Nerve supply of the

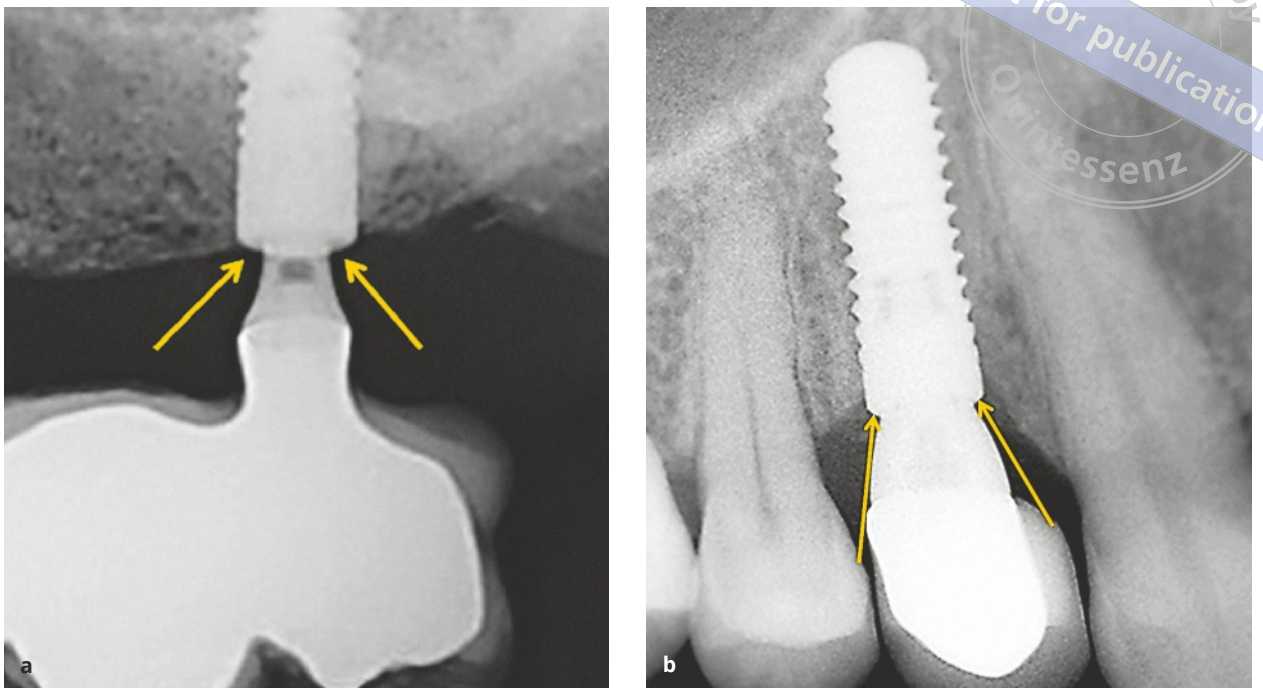

Figs 1-17a, b In cases where platform switching has been selected, the implant abutment leaves a significant width of the implant neck uncovered for the soft tissues to adhere to (yellow arrows). Thus, there is no need to proceed to bone resorption to give enough height for soft tissue adhesion.

gingiva and peri-implant mucosa is achieved with the sensory terminal branches of the second and third branches of the trigeminal nerve. Free nerve endings, responsible for pain and pressure, Meissner corpuscles, responsible for touch, Krause bulboid corpuscles (thermal receptors), as well as sympathetic and parasympathetic fibers, are responsible for vascular nerve supply.[19]

The lack of a periodontal membrane implies a significant absence of proprioperception and pressure sensing, which should be considered when designing implant restorations; the excessive application of pressure, during functional and parafunctional movements, may lead to technical complications. The sensation of pressure from the nerve endings of the osseous tissue is ten times smaller than that of the periodontal membrane.[20,21]

1.5 Biologic width around teeth and implants

Regarding biologic width, the following term has been suggested: "supracrestal tissue attachment" or "supracrestal attached tissues". This is defined as the distance between the most coronal termination of the junctional epithelium to the crest of the alveolar ridge. Its mean length is approximately 3 to 4 mm; it contains the width of the junctional epithelium and of the supracrestal connective tissue fibers that insert into the root cementum as Sharpey fibers. The soft tissue zone that attaches to the implant consists of approximately 2 mm junctional epithelium and 1 to 2 mm connective tissue, that is, a 3- to 4-mm width of soft tissue corresponds to the biologic width around teeth. Biologic width around submerged and non-submerged implants is similar regardless of functional loading.[22]

Due to non-submerged healing or after implant exposure of submerged healing, soft tissue attachment is established circumferentially to the implant neck. The stability of biologic width of soft tissues around implants has also been shown in animal studies. After the extraction of all premolars in the mandible, implants and healing abutments were placed. The mucosa on one side was thinned, while that of the opposing side remained untouched and was therefore left thicker. After 6 months and completion of the healing process, the attachment zone of the

soft tissues around both sides was 3.3 to 3.8 mm wide, consisting of 2.0 to 2.1 mm junctional epithelium and 1.3 to 1.8 mm connective tissue. At the site where the mucosa had initially been thinned, bone resorption of the alveolar ridge was noted to ensure the necessary 3to 4 mm soft tissue attachment.[23]

Finally, there was greater bone loss at the buccal site of the alveolar ridge compared to the lingual and palatal sites. Bone resorption to establish biologic width leads to deepening of the peri-implant crevice and is probably related to peri-implant inflammation. To contain bone resorption after connection of the implant abutment, platform switching has been recommended, that is, placement of a healing abutment with a smaller diameter than that of the cervical part of the implant (Figs 1-17a, b).[24] This method, however, poses one significant problem during the maintenance phase: it makes it impossible to evaluate differences between measurements of the depth of the peri-implant sulcus.

References

1. Nanci A, Bosshardt DD. Structure of periodontal tissues in health and disease. Periodontol 2000 2006;40:11–28.
2. Abrahamsson I, Berglundh T, Moon IS, Lindhe J. Peri-implant tissues at submerged and non-submerged titanium implants. J Clin Periodontol 1999;9:600–607.
3. Parpaiola A, Cecchinato D, Toia M, Bressan E, Speroni S, Lindhe J. Dimensions of the healthy gingiva and peri-implant mucosa. Clin Oral Implants Res 2015;26:657–662.
4. Weber HP, Buser D, Donath K, et al. Comparisons of healed tissues adjacent to submerged and non-submerged unloaded titanium dental implants. A histometric study in beagle dogs. Clin Oral Implants Res 1996;7: 11–19.
5. Berglundh T, Lindhe J, Ericsson I, Marinello CP, Liljenberg B, Thomsen P. The soft tissue barrier at implants and teeth. Clin Oral Implants Res 1991;2:81–90.
6. Tonetti MS, Gerber L, Lang NP. Vascular adhesion molecules and initial development of inflammation in clinically healthy human keratinized mucosa around teeth and osseointegrated implants. J Periodontal Res 1994;29: 386–392.
7. Schmid B, Spicher I, Schmid J, Lang NP. Plasminogen activator in human gingival tissue adjacent to dental implants. Clin Oral Implants Res 1992;3:85–89.
8. Glavind L, Zander HA. Dynamics of dental epithelium during tooth eruption. J Dent Res 1970;49:549–555.
9. Lindhe J, Berglundh T. The interface between the mucosa and the implant. Periodontol 2000 1998;17:47–54.
10. Abrahamsson I, Berglundh T, Wennström J, Lindhe J. The peri-implant hard and soft tissues at different implant systems. A comparative study in the dog. Clin Oral Implants Res 1996;7:212–219.
11. Buser D, Weber HP, Donath K, Fiorellini JP, Paquette DW, Williams RC. Soft tissue reactions to non-submerged unloaded titanium implants in beagle dogs. J Periodontol 1992;63:225–235.
12. Schroeder A, van der Zypen E, Stich H, Sutter F. The reactions of bone, connective tissue, and epithelium to endosteal implants with titanium-sprayed surfaces. J Maxillofac Surg 1981;9:15–25.
13. Abrahamsson I, Berglundh T, Glantz PO, Lindhe J. The mucosal attachment at different abutments. An experimental study in dogs. J Clin Periodontol 1998;25:721–727.
14. Cochran DL, Hermann JS, Schenk RK, Higginbottom FL, Buser D. Biologic width around titanium implants. A histometric analysis of the implanto-gingival junction around unloaded and loaded nonsubmerged implants in the canine mandible. J Periodontol 1997;68:186–198.
15. Moon IS, Berglundh T, Abrahamsson I, Linder E, Lindhe J. The barrier between the keratinized mucosa and the dental implant. An experimental study in the dog. J Clin Periodontol 1999;26:658–663.
16. Romanos GE, Schröter-Kermani C, Weingart D, Strub JR. Health human periodontal versus peri-implant gingival tissues: an immunohistochemical differentiation of the extracellular matrix. Int J Oral Maxillofac Implants 1995;10:750–758.
17. Egelberg J. The blood vessels of the dento-gingival junction. J Periodontal Res 1966;1:163–179.
18. Berglundh T, Lindhe J, Jonsson K, Ericsson I. The topography of the vascular systems in the periodontal and peri-implant tissues in the dog. J Clin Periodontol 1994;21:89–93.
19. Marchetti C, Poggi P, Reguzzoni M, Cornaglia AI, Baena YR. Lymphatic vessel system in gingival peri-implant tissues in humans. J Periodontal Res 1999;34:229–231.
20. Hämmerle CH, Wagner T, Brägger U, et al. Threshold of tactile sensitivity perceived with dental endosseous implants and natural teeth. Clin Oral Implants Res 1995;6:83–90.
21. Lindhe J, Berglundh T, Ericsson I, Liljenberg B, Marinello C. Experimental breakdown of peri-implant and periodontal tissues. A study in the beagle dog. Clin Oral Implants Res 1992;3:9–16.
22. Tarnow D, Hochman M, Chu S, Fletcher P. A new definition of attached gingiva around teeth and implants in healthy and diseased sites. Int J Periodontics Restorative Dent 2021;41:43–49.
23. Berglundh T, Lindhe J. Dimension of the peri-implant mucosa. Biological width revisited. J Clin Periodontol 1996;23:971–973.
24. Gupta S, Sabharwal R, Nazeer J, Taneja L, Choudhury BK, Sahu S. Platform switching technique and crestal bone loss around the dental implants: a systematic review. Ann Afr Med 2019;18:1–6.

2 Peri-Implant Tissue Healing after Implant Placement

2.1 Osseointegration

The term "osseointegration" is used to describe the direct structural and functional connection between living bone and the surface of a load-bearing artificial implant without intervening soft tissues, as can be observed under the microscope.[1] The term implies that elements foreign to the organism will be accepted by it and this integration will not be affected after their extended function over time (Fig 2-1).

The initial prerequisite for a foreign body to be integrated within the human organism is to not activate the immune response, causing a foreign body reaction after its placement. Biocompatible materials that satisfy this prerequisite are titanium and ceramic materials. Thus far, titanium alloys have proven to be the optimal choice due to their high resistance to corrosion and superior mechanical properties.[2] The TiO_2 and TiO_3 oxides form crystalline structures that rest on the implant surface and make it biologically inert. They are formed within 0.001 seconds after exposure of titanium to air, biologic fluids, water, or electrolytes.

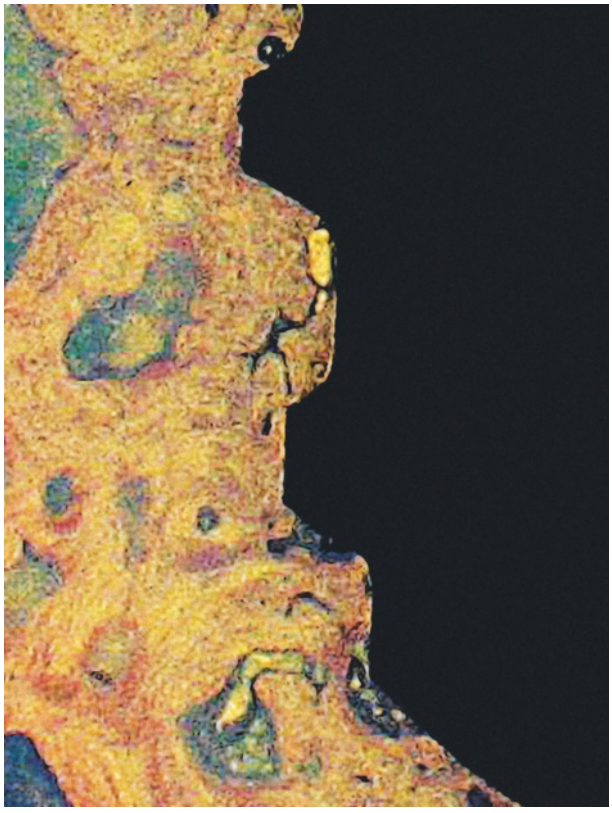

Fig 2-1 Detail of a histologic analysis derived from the maxilla of a dog, where mature osseous tissue in direct structural and functional contact with an implant may be observed. The implant had accepted functional loading for a significant amount of time before the animal was sacrificed (courtesy of Mr L. Podaropoulos, and Drs P. Trisi and D. Kalyvas).

2.2 From bed preparation to osseointegration

During implant placement in an edentulous area, trauma is caused to the underlying bone that is drilled to prepare the bed that will host the implant. In the bone, specifically at the borders of the canal that is prepared, a limited necrotic zone is formed, while bone fragments remain at the preparation site.

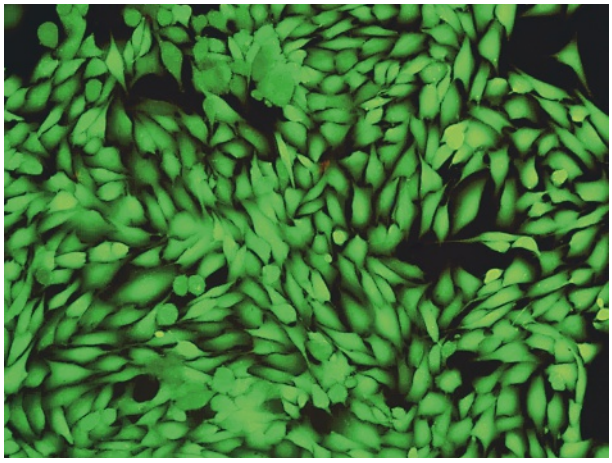

Fig 2-2 Image from fluorescence microscopy (×20 magnification) of immature osteoblasts, MG63, cultured for 48 hours after being irradiated with low-level laser energy to promote cell proliferation, using an Nd:YAG laser (1,064 nm).

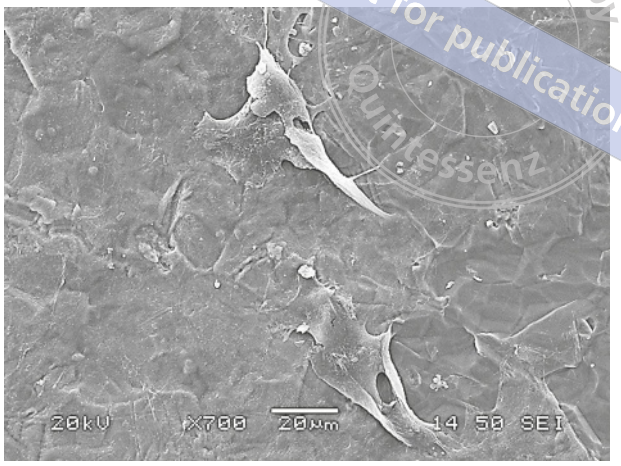

Fig 2-3 Micrograph (×700 magnification) of immature osteoblasts cultured on smooth titanium surfaces for 7 days.

This trauma triggers the healing mechanism. A series of events follow that ultimately lead to the formation of new osseous tissue.

To achieve primary stability, the preparation is made so that its perimeter is slightly smaller than that of the implant. The implant is then inserted so that its threads are 0.5 to 1.0 mm below the borderline of the bed preparation. The pressure applied to screw the implant in crushes the blood vessels, leading to hemorrhage and the formation of a blood clot between the bone and the implant surface.[3] Osteoblasts, cells capable of forming new osseous tissue, are crucial for the healing process. Osteoclasts, multinuclear cells derived from blood monocytes that induce bone resorption, and osteocytes, which participate in osteolytic processes, are also essential. In addition, undifferentiated mesenchymal cells play a key role because they are multipotent and, depending on the stimulus, may differentiate into pre-osteoblasts and later osteoblasts (Figs 2-2 and 2-3).

Occasionally, however, these cells may differentiate into fibroblasts, making osseointegration impossible. For optimal cell function and to trigger the onset of the healing process, sufficient blood supply to the area and formation of new microcirculation are necessary. The speed at which new vessels are created differs significantly between cortical and trabecular bone. For the latter, this process proceeds at a rate of 0.5 mm per day; this is slower for cortical bone, proceeding at 0.05 mm per day. The blood clot created matures over the first few days after surgery and is gradually replaced with granulation tissue replete with neutrophils and monocytes, while white blood cells simultaneously remove necrotic elements at the site. Newly formed vessels begin to organize into granulation tissue.[4]

Three stages of osseointegration have been identified:[5]

- woven bone formation;
- parallel fiber and lamellar bone deposition;
- bone remodeling.

A brief description of the series of events from the day of implant insertion to the development of osseointegration follows.[5]

On the first day after implant placement, its stability may be solely attributed to the mechanical retention achieved by the threadlike (spiral) shape of the implant or pressed fit or friction fit and depends on the size and density of the threads, the precision in bed preparation, and bone type (cortical or trabecular). At this stage, the implant–bone contact, which reaches 35% when observed histomorphometrically, does not constitute osseointegration. The implant surface is mainly in contact with parts of the cortical and trabecular bone that were detached during preparation, with a blood clot or, at the peak of the threads, with condensed trabecular bone due to the screwing process. Multinuclear giant cells and macrophages may also be apparent.

Three days after implant placement, there is significant migration of mesenchymal cells and macro-

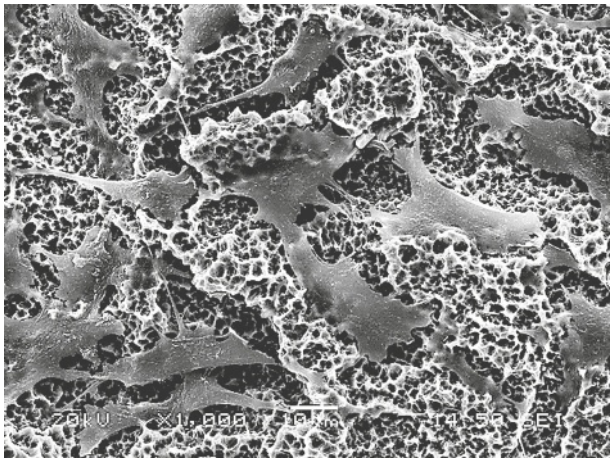

Fig 2-4 Micrograph (×1,000 magnification) showing a strong contact between the body and filopodia of the osteoblasts and the titanium surface 7 days after culturing. An irregular shape of the cells may observed.

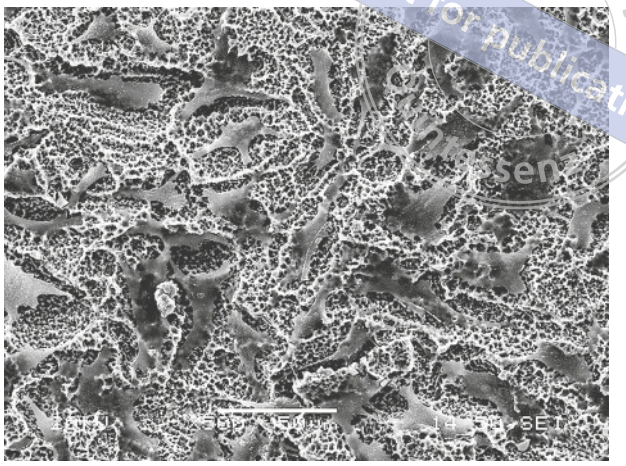

Fig 2-5 Micrograph (×500 magnification) of immature osteoblasts cultured on a rough titanium surface (sandblasted, acid-etched, Straumann) for 7 days. The irregular shape of the cells is evident, as well as the contact between the body and filopodia of the cells with the titanium surface.

phages from the bone marrow to the blood clot between the bone and the implant. The bone–implant contact proportion is stable but this is still due to mechanical retention. There is also development of granulation tissue and the first newly formed capillary vessels. Moreover, collagen fibers may be observed.

Seven days later, production of woven bone can be observed. Woven bone has a similar orientation to that of collagen fibers, that is, perpendicular to the implant surface, and may be used as a matrix to produce osteoid clones from osteoblasts. As time passes, the formed bone occupies the space around the implant threads, increasing the bone–implant contact to around 50% of the implant surface. This newly formed woven bone is circumferentially arranged into a dense net of blood vessels, which had already been established at the peri-implant area, and is characterized by many irregularly shaped osteoblasts (Fig 2-4).

Gradual shaping of a network takes place, which consists of formations that look like sticks and plates. This network expands into the surrounding space at a relatively rapid pace. Woven bone is deposited at a remarkable rate of 30 to 50 µm per day. In contrast to mature osseous tissue, the concentration of inorganic elements is initially low. The fibers of the matrix are randomly ordered and resistance to mechanical strain is low. In areas where there is a lack of implant–bone contact, a layer of multinuclear giant cells may be found, which is retained even though the number of giant cells gradually decreases.

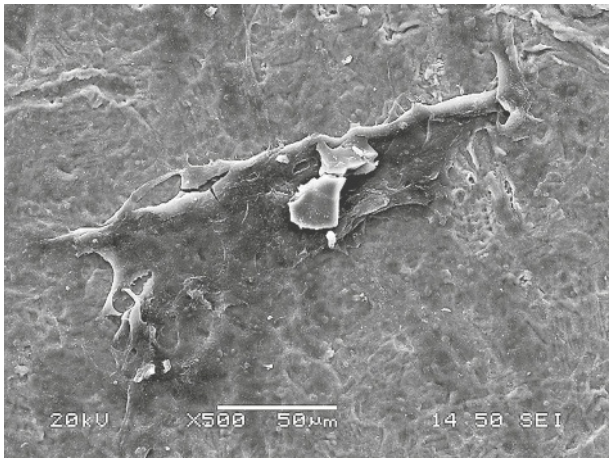

Fig 2-6 Micrograph (×500 magnification) of immature osteoblasts cultured on a smooth titanium surface for 7 days. The irregular shape of the cells may be noted, as well as the relatively weak contact of the cell body and filopodia with the titanium surface, compared to the contact on a rough surface.

From this point onward, all events are significantly affected by the type of implant surface and whether or not this surface has been processed so that its biologic behavior promotes the acceleration of osseointegration (Figs 2-5 and 2-6).

In general, during the first 14 days, woven bone begins to be replaced by lamellar or parallel fiber bone through the osteoclastic process. Mature lamellar bone is characterized by high resistance to mechanical strain (Fig 2-7).

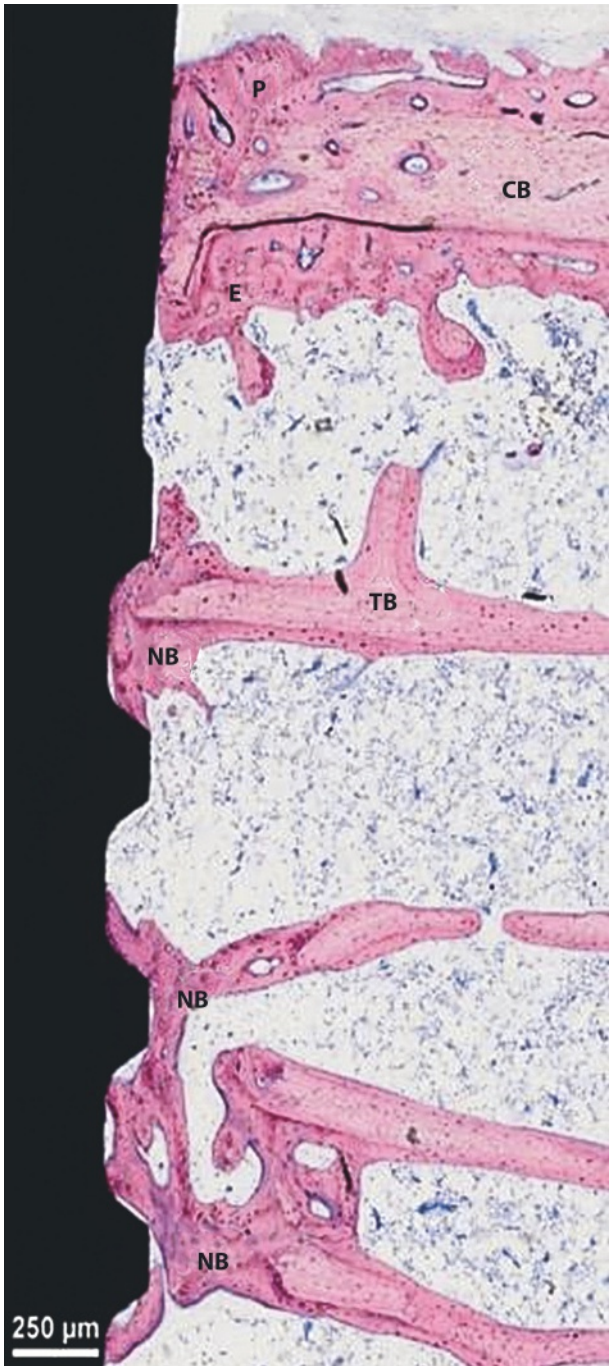

Fig 2-7 The preexisting bone can be divided into cortical (CB) and trabecular (TB). The newly formed bone (NB), which is the result of processes that take place after implantation, may be divided into endosseous (E) and periosteal (P). Levai Laczko staining (Fig 23, page 82 of the thesis by Tsetsenekou[6] reproduced with permission from the author).

As mentioned, the rate of deposition of this type of osseous tissue depends on the type of implant surface and how it is treated. For implants with low roughness, a production rate of 1.0 to 1.5 µm per day has been reported and complete osseointegration is achieved in 22 to 24 weeks. Even though replacement of woven bone in smooth implants may last up to 6 months in the maxilla, improvement of the implant surface characteristics may reduce the time required for complete osseointegration. Research has shown that the time needed is 6 weeks for implants with sandblasted, large-grit, and acid-etched (SLA) surfaces; this may be reduced to 3 weeks for implants with nano-modified implant surfaces (SLActive, sandblasted, large-grit, and acid-etched plus chemically activated) (Figs 2-8 to 2-10a). Once the process is completed (the length of time differs depending on the characteristics of the surface of the implant), the rate of implant–bone contact reaches 70%, corresponding to true osseointegration. The effect of the roughness of the implant surface on osseointegration will be analyzed further in this chapter.

2.3 Bone remodeling

The third and final stage of osseointegration is the lifelong process of bone remodeling (bone resorption followed by bone deposition), which corresponds to changes in functional loading applied to the implant. Remodeling begins at around the third month after implant placement. It is characterized by an initial period of increasing osteoclast activity that lasts for several weeks and gradually decreases, while remaining in function throughout the life of the patient. Bone remodeling is extremely important not only to maintain osseointegration, but also to preserve the functional integrity of the whole skeleton. Through the replacement of woven bone with mature, lamellar bone, the quality of the osseous tissue is improved (Fig 2-10b).

The peri-implant bone endures fatigue due to constant loading. Despite bone remodeling, the accumulation of damage caused by constant loading, may in rare instances lead to aseptic necrosis. During initial bone deposition, primary osteons are formed; during bone remodeling, secondary osteons are created. Initially, there is bone resorption through osteoclasts that results in a cylindrical canal, with an

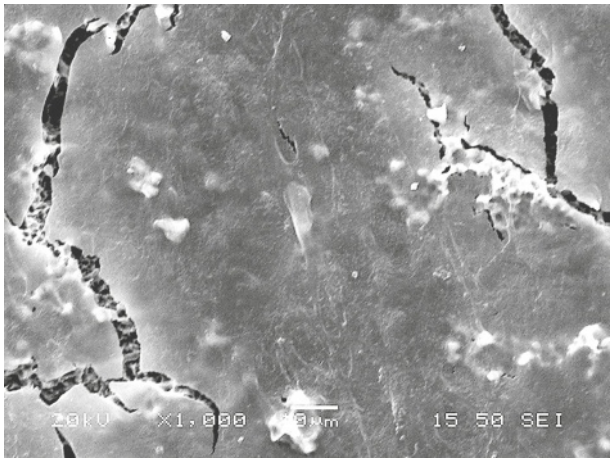

Fig 2-8 Micrograph (×1,000 magnification) of osteoblasts cultured on rough titanium surfaces (sandblasted, acid-etched, Straumann) for 3 weeks. A dense layer of osteoids on the rough surface may be observed.

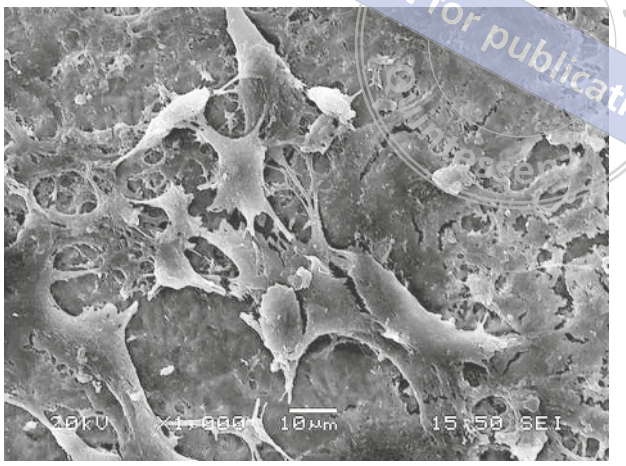

Fig 2-9 Micrograph (×1,000 magnification) of osteoblasts cultured on smooth titanium surfaces for 3 weeks. Cell proliferation is significant on a smooth surface yet it does not result in the formation of a dense layer of osteoids, as is the case on rough surfaces.

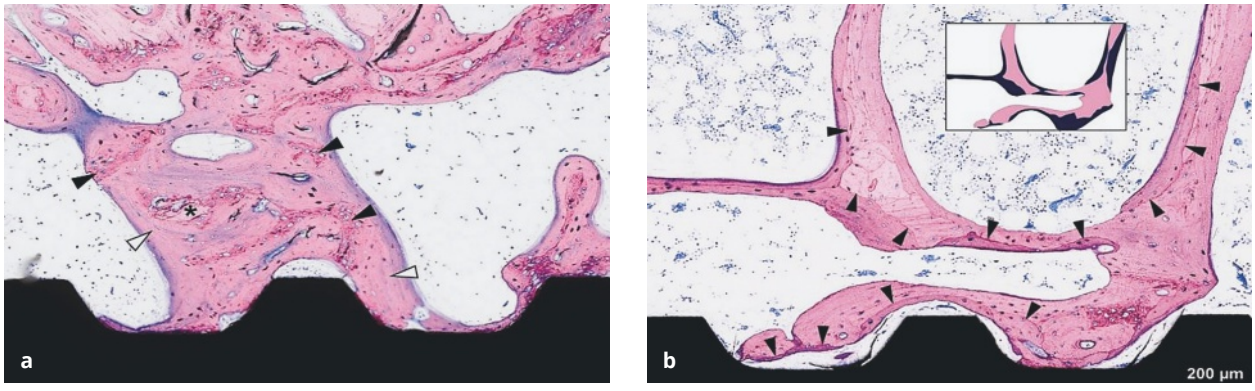

Figs 2-10a, b Quality and synthesis of peri-implant osseous tissue. **(a)** After 6 weeks, the osseous tissue at the area of the mesophase consists of a mesh of woven (black arrows) and lamellar (white arrows) bone. **(b)** After 12 weeks, a significant proportion of this complex bone was replaced with lamellar bone (dark blue areas) amid the procedure of bone remodeling. Inversion lines marked with black arrows indicate the remodeling process (Lavai Laczko staining) **(b)** (Fig 27, page 86 of the thesis by Tsetsenekou[6]; reproduced with permission from the author).

osteon diameter of 150 to 200 µm. The canal is gradually filled with newly formed bone that is deposited by osteoblasts. The bone is deposited in the form of concentric rings. Formation of a new osteon takes up to 2 to 4 months. This process is similar to that of trabecular bone, where osteoclasts gather and leave a corrosive cavity behind that is filled with lamellar bone at approximately 2 weeks. Interestingly, the rate of physiologic remodeling around a functional implant is two to ten times greater than that noted in other areas of the body (Figs 2-11 and 2-12).[7]

2.4 The influence of implant surface configuration on osseointegration

A series of in vitro studies conducted in the 1980s that examined a plethora of factors affecting the success of implant therapy concluded that surface topography had a statistically significant effect on the process of osseointegration. The reason for this was

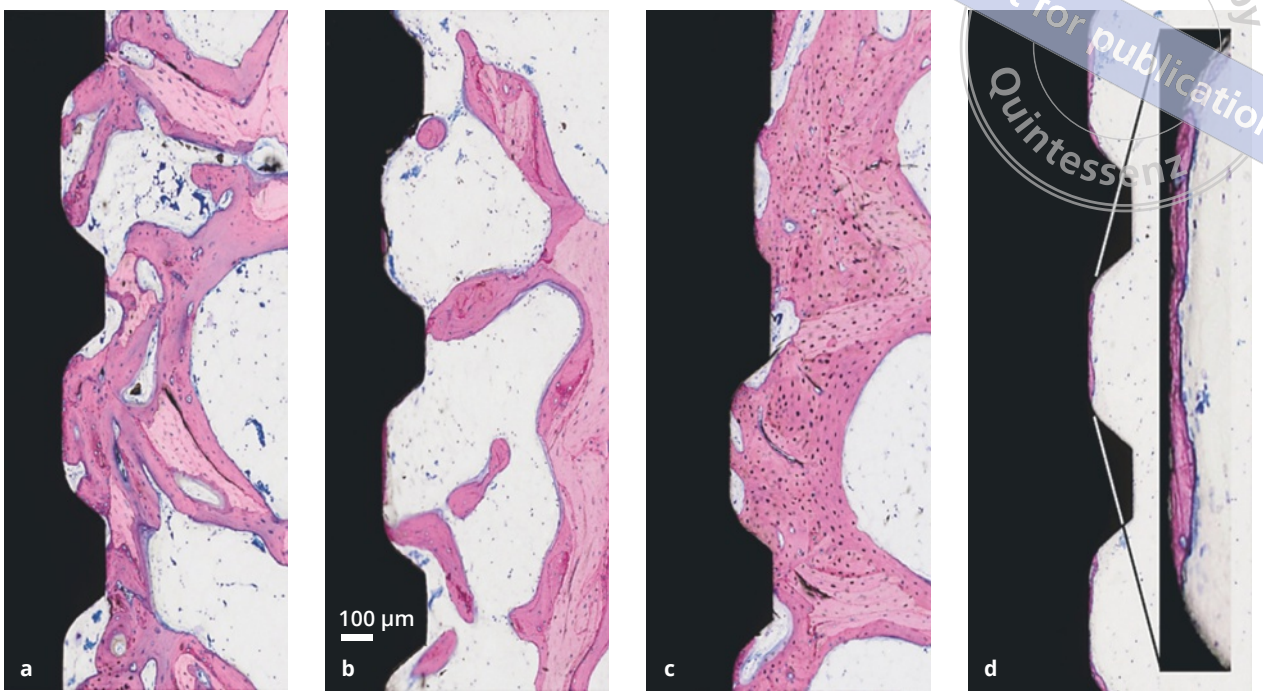

Figs 2-11a–d Different types of bone formation in the bone–implant mesophase. **(a)** The newly formed tissue extends from the preexisting one and covers the implant and adjacent trabeculae. **(b)** Annular forms of new osseous tissue. **(c)** New bone is deposited in wide layers. **(d)** Strips of woven bone (Levai Laczko staining) (Fig 24, page 84 of the thesis by Tsetsenekou[6]; reproduced with permission from the author).

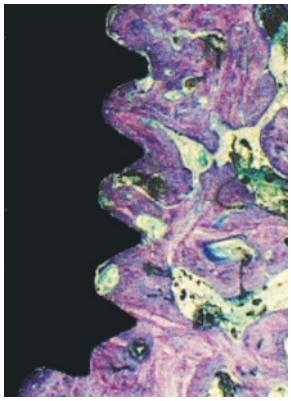

Fig 2-12 Histologic image depicting the direct contact of lamellar bone with the implant surface, which undergoes functional loading with great force (courtesy of Drs L. Podaropoulos, P. Trisi, and D. Kalyvas).

that the nature of a biomaterial, as well as its physical and chemical properties, influence the formation of steady adhesion of the bone to the implant.

Mechanical treatment of a titanium surface (machined surface) and anodic oxidization produce relatively smooth surfaces (Figs 2-13a, b to 2-15).

Surface roughness may be achieved with subtractive, prosthetic, or coating methods. Subtractive methods include treatment with a strong acid or laser, and abrasion with TiO_2 or Al_2O_3 particles of various diameters (such as SLA), whereas prosthetic methods consist of titanium plasma spraying (TPS) and hydroxyapatite coating (Figs 2-16a, b to 2-20).

Histologically, the initial contact between the bone and implant covered with TPS may be achieved just a week after placement. On the other hand, the initial bone contact with an implant with a smooth surface has been observed 3 weeks after placement. In most cases, formation of a blood clot was noted in a tight formation around the microrough surface of TPS implants, which has been attributed to the better retention of the fibrin mesh created during the blood clotting. The connection between the fibrin mesh and the implant surface is a decisive event; it is used as a scaffold for osteoprogenitor cells to migrate toward the implant. For this connection to be stable, primary stability of the implant during its mechanical retention in the implant bed must first be achieved; uncontrolled force application that could lead to its early failure must be avoided (Figs 2-21a–d).

In the years that followed, several in vivo studies compared the rate of bone–implant contact (Fig 2-22) between smooth surfaces and surfaces treated to become rougher. Histologic evaluation was performed between 3 weeks and 1 year and showed more rapid deposition of new bone on roughened surfaces com-

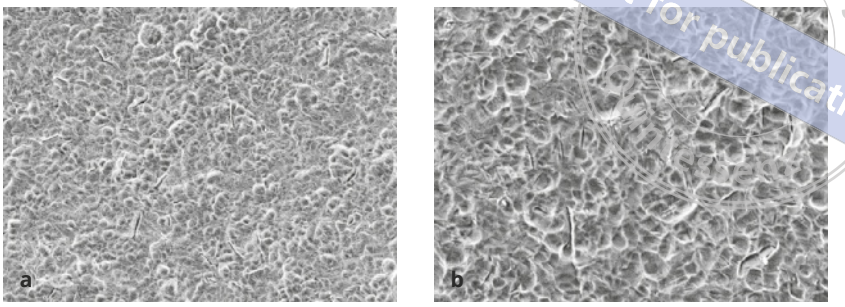

Figs 2-13a, b Polished titanium surface. **(a)** ×500 magnification. **(b)** ×1,000 magnification.

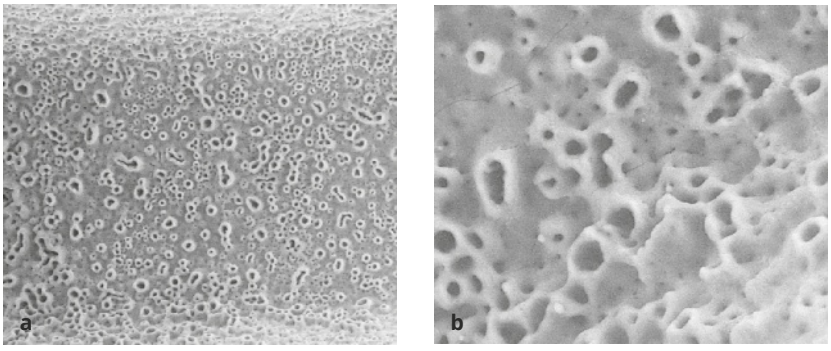

Figs 2-14a, b Scanning electron micrographs. **(a)** Rough surface that has undergone anodic oxidization (Nobel Biocare) at ×600 magnification. **(b)** The same micrograph at ×2,400 magnification (courtesy of Drs T. Papadopoulos and I. Fandrides).

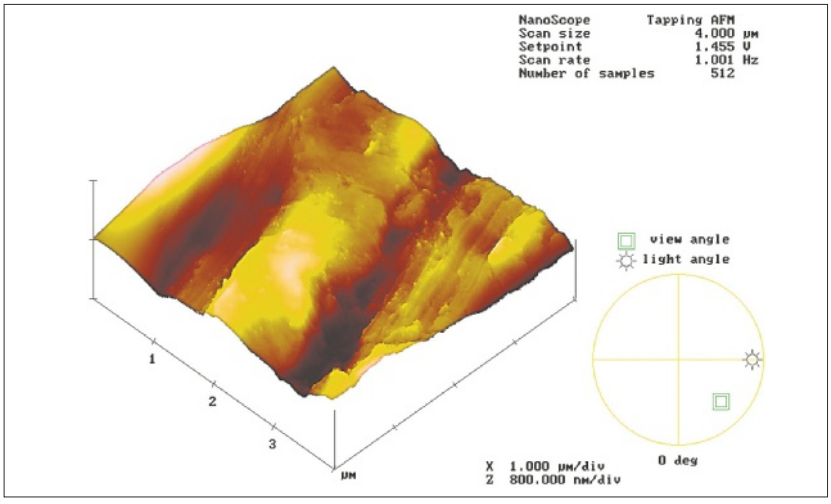

Fig 2-15 Application of atomic force microscopy revealed the low roughness of a smooth surface (Nobel Biocare), which promotes the adhesion of epithelial cells through hemidesmosomes (courtesy of Drs T. Papadopoulos and I. Fandrides).

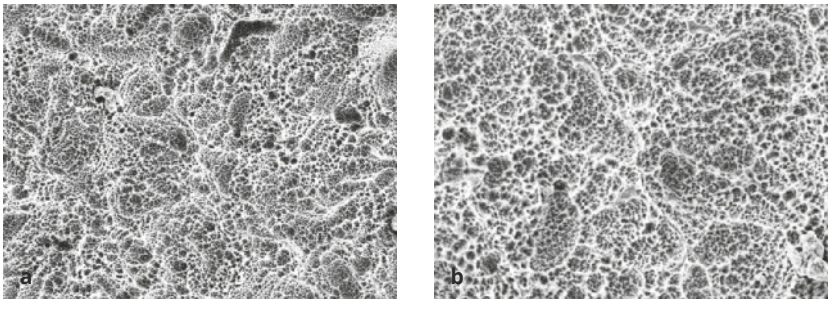

Figs 2-16a, b Titanium surface that has undergone treatment with airborne-particle abrasion and acids (Straumann) as can be seen in the micrographs. **(a)** ×500 magnification. **(b)** ×1,000 magnification.

pared to smooth surfaces, leading to an increased rate of bone–implant contact for these surfaces. Specifically, after 6 weeks of healing, the highest rate of bone–implant contact was noted around implants with an SLA surface (50% to 60%) and those with an hydroxyapatite coating (60% to 70%). In descending order, large-grit airborne-particle abraded surfaces follow (30% to 40%), as well as surfaces that under-

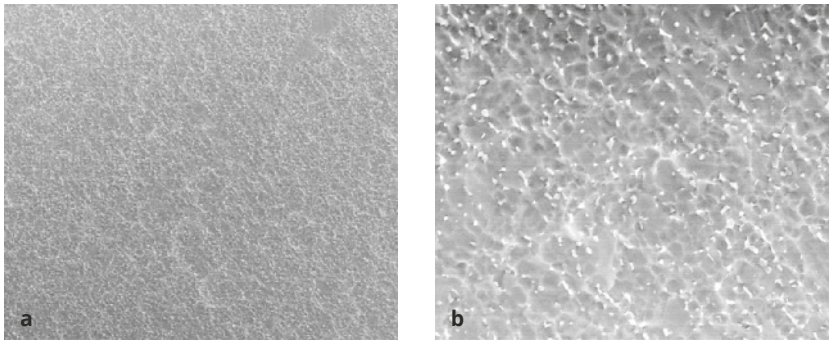

Figs 2-17a, b Micrographs. **(a)** Rough surface that has undergone airborne-particle abrasion with Al_2O_3 grains and chemical etching (MIS) at ×600 magnification. **(b)** the same micrograph at ×2,400 magnification (courtesy of Drs T. Papadopoulos and I. Fandrides).

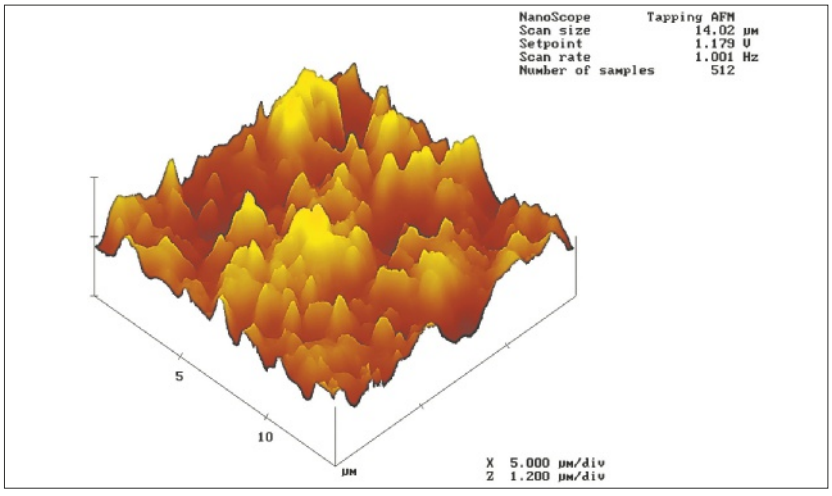

Fig 2-18 Application of atomic force microscopy revealed the roughness of a rough surface (MIS, Misgav, Israel) (courtesy of Drs T. Papadopoulos and I. Fandrides).

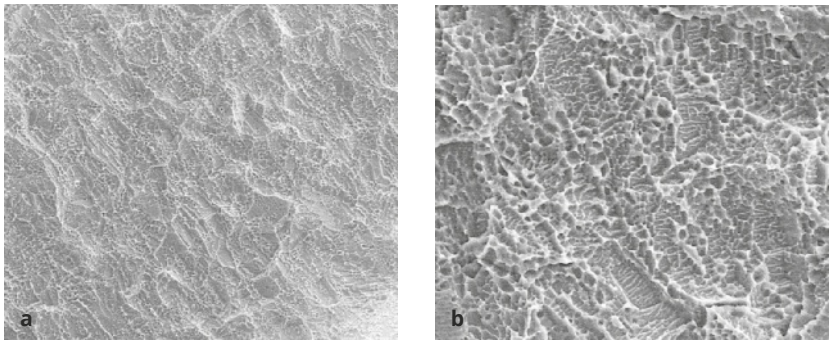

Figs 2-19a, b Micrographs. **(a)** Rough surface that has undergone chemical etching with 15% hydrofluoric acid and H_2SO_4/HCl (6:1) at 60°C to 80°C for 3 to 10 minutes (3i) at ×600 magnification. **(b)** The same micrograph at ×2,400 magnification (courtesy of Drs T. Papadopoulos and I. Fandrides).

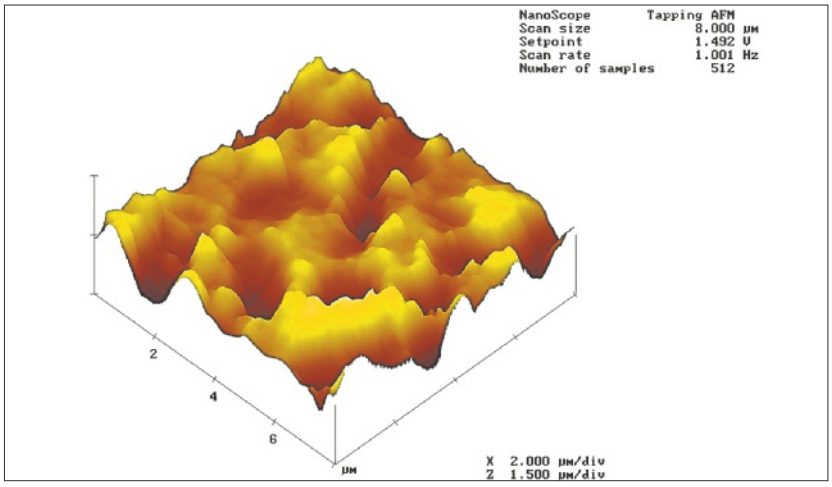

Fig 2-20 Application of atomic force microscopy revealed the roughness of a rough 3i surface (courtesy of Drs T. Papadopoulos and I. Fandrides).

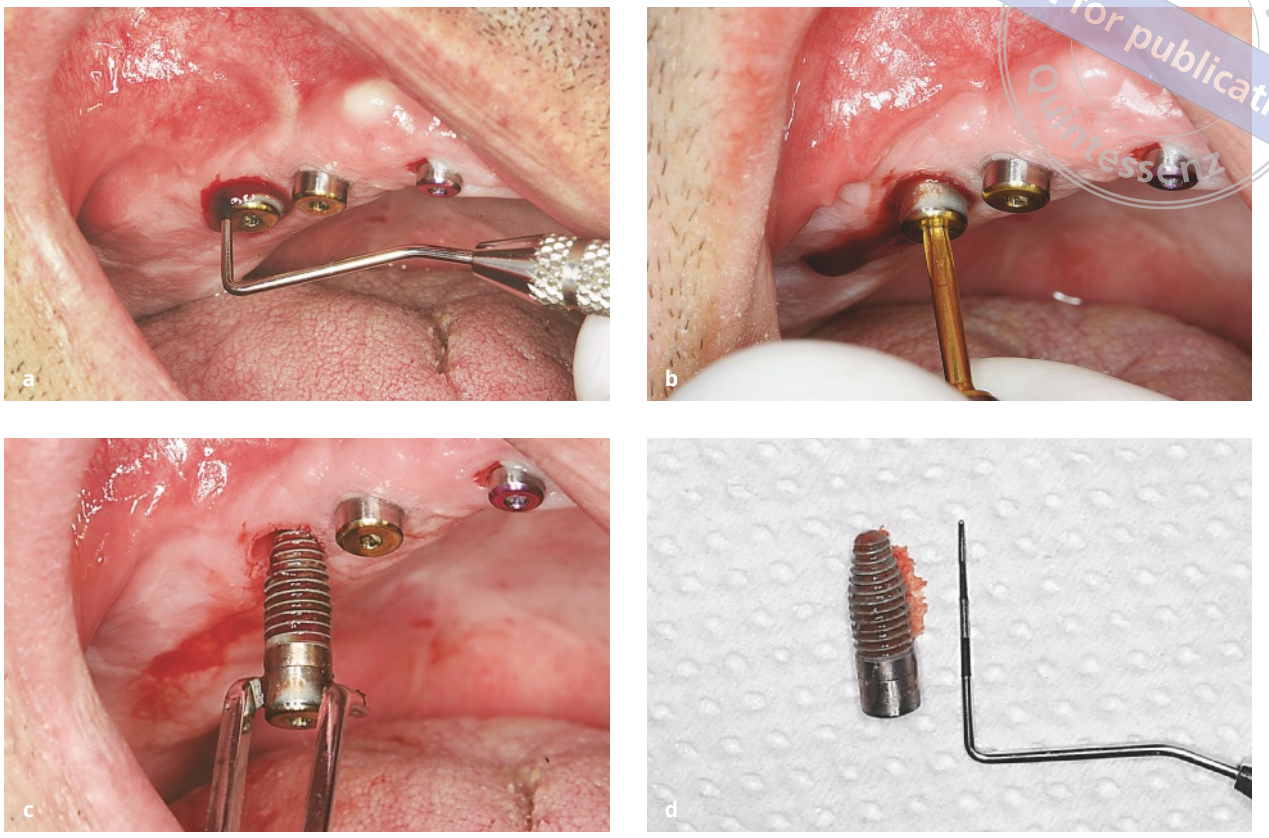

Figs 2-21a–d The loss of this implant was attributed to the failure of osseointegration due to excessive application of force from a complete denture provisional prosthesis.

go airborne-particle abrasion with medium-sized grits, and, finally, machined surfaces (20% to 25%). Implants coated with hydroxyapatite (HA) often show signs of resorption or detachment of their external coat.[7] Notably, surfaces that have undergone treatment with airborne-particle abrasion and acids became hydrophilic, and show improved bone–implant contact. This is achieved by the role of the modified SLA surface in cellular differentiation and production of growth factors. Modification of the SLA surface is achieved with treatment in a nitrogen environment (N_2); the implant is stored in a package that contains an isotonic solution. Thus, the surface is hydrated and the hydroxyl group connections are increased. Only small quantities of hydrogen carbonates and carbon remain on the surface. These implants may be loaded just 3 weeks after placement.[9-17]

A comparison of implants with treated versus smooth surfaces, with regard to the torque removal force, showed that treated surfaces require greater forces to be loosened from the bone. Those studies were performed in guinea pigs and in bone with a different density than human bone. However, the greatest torque removal forces were achieved for TPS or SLA surfaces.[18]

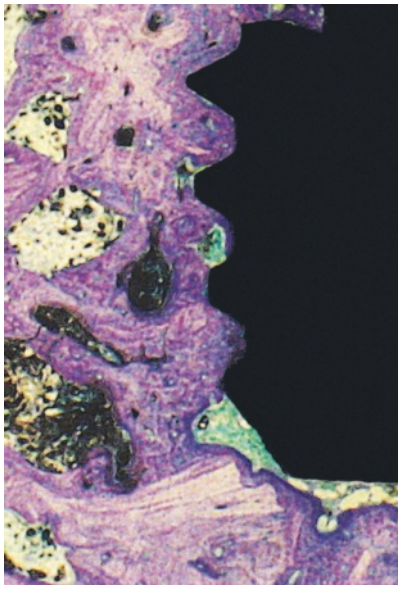

Fig 2-22 The percentage of contact between osseous tissue (not trabeculae) in linear measurements along the implant surface was used to express the quality of osseointegration (bone–implant contact). In this case, a high percentage of bone–implant contact has been achieved (courtesy of Drs L. Podaropoulos, P. Trisi, and D. Kalyvas).

At the cellular level, the reaction of peri-implant tissues is influenced by the topography of each surface, not only at the level of metabolic activity, but also as far as adhesion to it is concerned. In vitro experiments on TPS or SLA surfaces versus smooth surfaces have shown that osteoblast-like cells in contact with rough surfaces produce up to four times more prostaglandin E2 and tumor growth factor β1. This increased production of biologic mediators suggests that rougher surfaces may lead to alterations in cellular activity and consequently affect healing of the peri-implant bone. Equivalent conclusions have been reached for hormones such as osteocalcin and enzymes such as alkaline phosphatase.[19,20]

Moreover, apart from an increase in metabolic activity, surface topography affects the shape and arrangement of cells. In vitro studies have shown that the length, orientation, and adhesion level of osteoblasts is defined, to a great extent, by the texture of the surface they adhere to. In addition, an increase in osseous tissue production has been noted, with orientation corresponding to the microstructure of the surface. Specifically, osteoblast adhesion is better in rough titanium surfaces, where a greater degree of extracellular matrix and higher salination are present.[21,22]

In conclusion, all interactions between peri-implant tissues and rough surfaces favorably influence the osseointegration process through the faster deposition of new bone, wider bone–implant contact, and greater removal torque.

A catalytic role in the achievement of osseointegration is played by adhesion of plasma proteins to the titanium surface, even though the exact process during trauma healing that leads to bone–implant contact is not yet clear. An additional element thought to play a crucial role is the neoangiogenesis created by the capillary vessels in the area. These cells, as undifferentiated mesenchymal cells, generate osteoblast precursor cells, which in turn lead to increased production of osteoblasts. This eventually leads to a positive effect on osseointegration.

References

1. Brånemark PI, Adell R, Breine U, Hansson BO, Lindström J, Ohlsson A. Intra-osseous anchorage of dental prostheses. I. Experimental studies. Scand J Plast Reconstr Surg 1969;3:81–100.
2. Steinemann S. The properties of titanium. In: Schroeder A, Sutter E, Buser D, Krekeler G (ed). Oral implantology. Basics, ITI Dental Implant System, ed 2. New York: Thieme Medical Publishers, 1996;37–59.
3. Javed F, Ahmed HB, Crespi R, Romanos GE. Role of primary stability for successful osseointegration of dental implants: factors of influence and evaluation. Interv Med Appl Sci 2013;5:162–167.
4. Davies JE. Understanding peri-implant endosseous healing. J Dent Educ 2003;67:932–949.
5. Schenk RK, Buser D. Osseointegration: a reality. Periodontol 2000 1998;17:22–35.
6. Tsetsenekou E. Histological and histomorphometrical evaluation of the osseointegration of nanotreated dental implants in New Zealand Rabbits under alendronate therapy. PhD Thesis, Athens, 2011.
7. Chappard D. Bone modeling and remodeling during osseointegration [in French]. Rev Stomatol Chir Maxillofac Chir Orale 2013;114:159–165.
8. Buser D, Shenk RK, Steinemann S, Fiorellini JP, Fox CH, Stich H. Influence of surface characteristics on bone integration of titanium implants. A histomorphometric study in miniature pigs. J Biomed Mater Res 1991;25:889–902.
9. Carr AB, Beds DW, Larsen PE. Reverse-torque failure of screw-shaped implants in baboons after 6 months of healing. Int J Oral Maxillofac Implants 1997;12:598–603.
10. Claes L, Hutzschenreuter P, Pohler O. The dependence of the removal torque of a leg screw surface and implantation time [in German]. Arch Orthop Unfallchir 1976;85:155–159.
11. Cochran DL, Schenk RK, Lussi A, Higginbottom FL, Buser D. Bone response to unloaded and loaded titanium implants with a sandblasted and acid-etched surface: a histometric study in the canine mandible. J Biomed Mater Res 1998;40:1–11.
12. Gotfredsen K, Nimb L, Hjörting-Hansen E, Jensen JS, Holmén A. Histomorphometric and removal torque analysis for smooth and TiO2-blasted titanium implants. An experimental study on dogs. Clin Oral Implants Res 1992;3:77–84.
13. Gotfredsen K, Wennerberg A, Johansson C, Skovgaard LT, Hjørting-Hansen E. Anchorage of TiO2-blasted, HA-coated, and machined implants: an experimental study with rabbits. J Biomed Mater Res 1995;29:1223–1231.
14. Bosshardt DD, Chappuis V, Buser D. Osseointegration of titanium, titanium alloy and zirconia dental implants: current knowledge and open questions. Periodontol 2000 2017;73:22–40.

15. Stafford GL. Review found little difference between sandblasted and acid-etched (SLA) dental implants and modified surface (SLActive) implants. Evid Based Dent 2014;15:87–88.
16. Smeets R, Stadlinger B, Schwarz F, et al. Impact of dental implant surface modifications on osseointegration. Biomed Res Int 2016;2016:6285620.
17. Carlsson L, Röstlund T, Albrektsson B, Albrektsson T. Removal torques for polished and rough titanium implants. Int J Oral Maxillofac Implants 1988;3:21–24.
18. Buser D, Nydegger T, Oxland T, et al. Interface shear strength of titanium implants with a sandblasted and acid-etched surface: a biomechanical study in the maxilla of miniature pigs. J Biomed Mater Res 1999;45: 75–83.
19. Lincks J, Boyan BD, Blanchard CR, et al. Response of MG63 osteoblast-like cells to titanium and titanium alloy is dependent on surface roughness and composition. Biomaterials 1998;19:2219–2232.
20. Martin JY, Schwartz Z, Hummert TW, et al. Effect of titanium surface roughness on proliferation, differentiation, and protein synthesis of human osteoblast-like cells (MG63). J Biomed Master Res 1995;29:389–401.
21. Lagonegro P, Trevisi G, Nasi L, et al. Osteoblasts preferentially adhere to peaks on micro-structured titanium. Dent Mater J 2018;37:278–285.
22. de Oliveira GJPL, Aroni MAT, Pinotti FE, Marcantonio E Jr, Marcantonio RAC. Low-level laser therapy (LLLT) in sites grafted with osteoconductive bone substitutes improves osseointegration. Lasers Med Sci 2020;35:1519–1529.

3 Classification of Peri-Implant Diseases

The classification of peri-implant diseases and defects is necessary for communication between clinics not only regarding diagnosis and prognosis, but also for a better understanding of the etiological factors involved. In addition, establishing the correct diagnosis helps the clinician to provide the appropriate treatment. Since the early 1990s, experts around the world have agreed to distinguish between two disease entities that affect peri-implant tissues, namely peri-implant mucositis and peri-implantitis. Additional denominators were proposed at the World Workshop on the Classification of Periodontal and Peri-Implant Diseases and Conditions in 2017. The description of health in particular was added:

- **Healthy peri-implant tissues** are characterized clinically and histologically by the absence of signs of inflammation. No bleeding on light probing is observed, even in cases of implants with reduced residual bone support (Figs 3-1 to 3-4a, b).
- **Peri-implant mucositis** is a reversible disease that has a microbial etiology; it is characterized by visible signs of inflammation and bleeding on probing (BOP). The disease is similar to gingivitis for natural dentition (Fig 3-5). Peri-implant mucositis can be treated by removing the main causative factor, namely the microbial biofilm, previously known as dental plaque. According to the 2017 classification, it is a reversible form of inflammation that occurs in the peri-implant mucosa after functional loading.[1] However, inflammation of the soft peri-implant tissues may be induced immediately by placing the implant using a single-phase protocol or uncovering if it was placed using a two-stage protocol. Because inflammation is limited to the soft tissues and is not a condition involving early implant failure, its topography and etiology classify it as peri-implant mucositis. Therefore, it

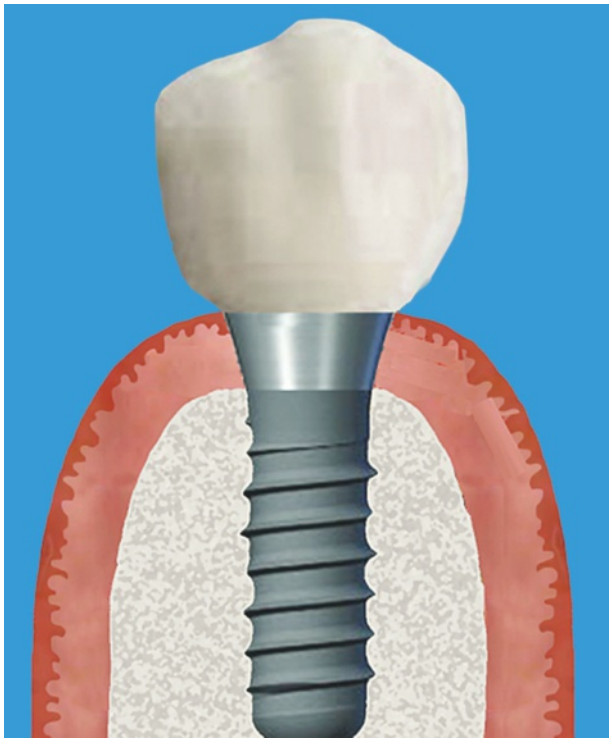

Fig 3-1 Schematic representation of healthy peri-implant tissues. No inflammation or bone loss is observed.

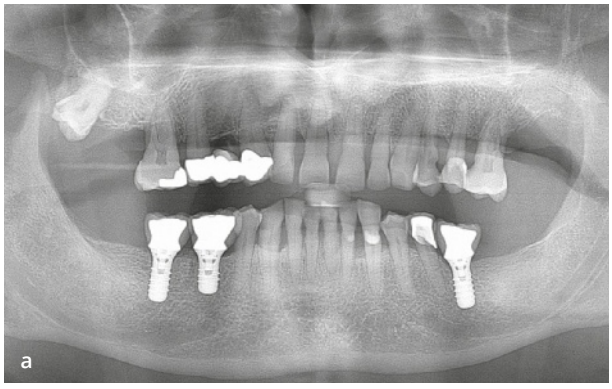

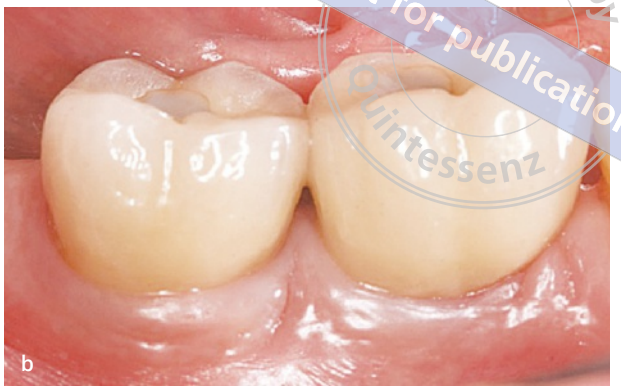

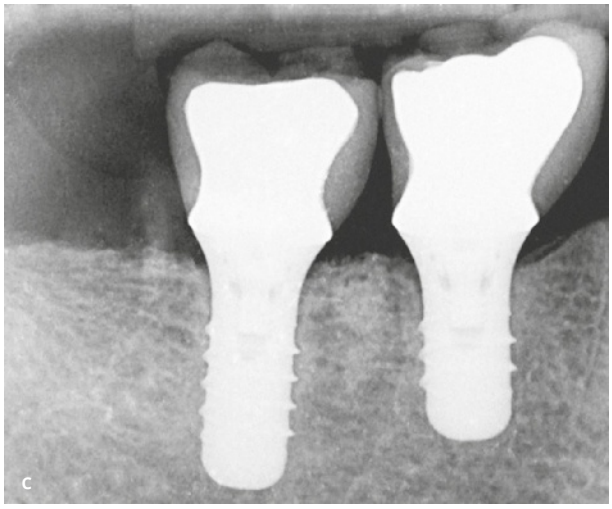

Figs 3-2a–c **(a)** Radiographic image of a patient after implant placement. **(b and c)** Clinical and radiographic images of healthy peri-implant tissues 6 years after placement of the implant-supported crowns. Note the absence of BOP, pockets, and bone loss.

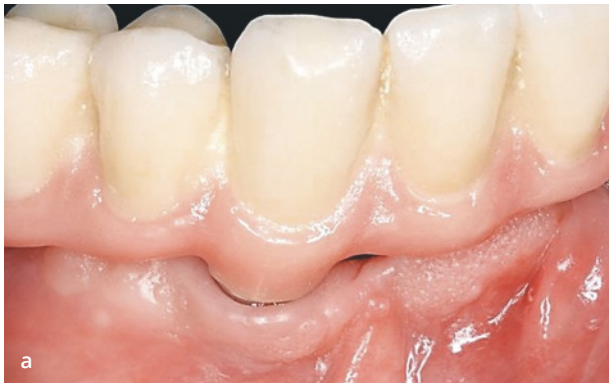

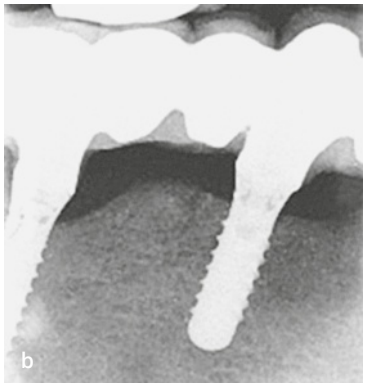

Figs 3-3a, b Clinical and radiographic images of healthy peri-implant tissues 8 years after implant placement. Note the absence of inflammation on probing, pockets, and bone loss.

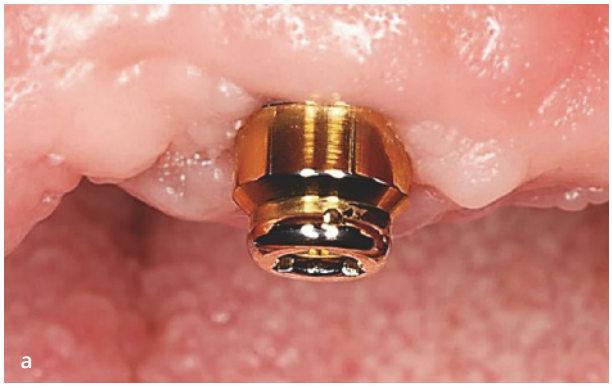

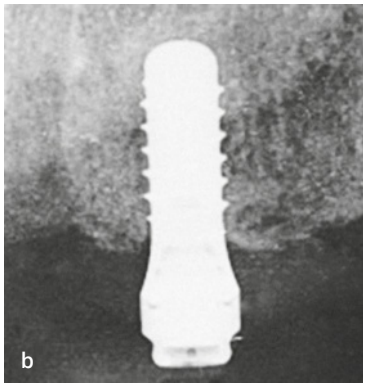

Figs 3-4a, b Clinical and radiographic images of healthy peri-implant tissues 7 years after incorporation of the denture. Note the absence of signs of inflammation and bone destruction.

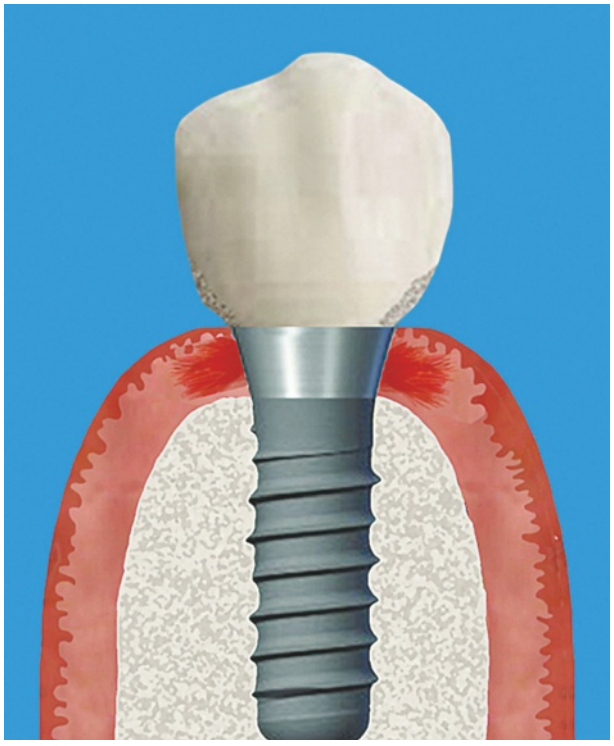

Fig 3-5 Schematic representation of peri-implant mucositis. Inflammation is limited to the peri-implant mucosa. There is no bone loss, while microbial biofilm is detected.

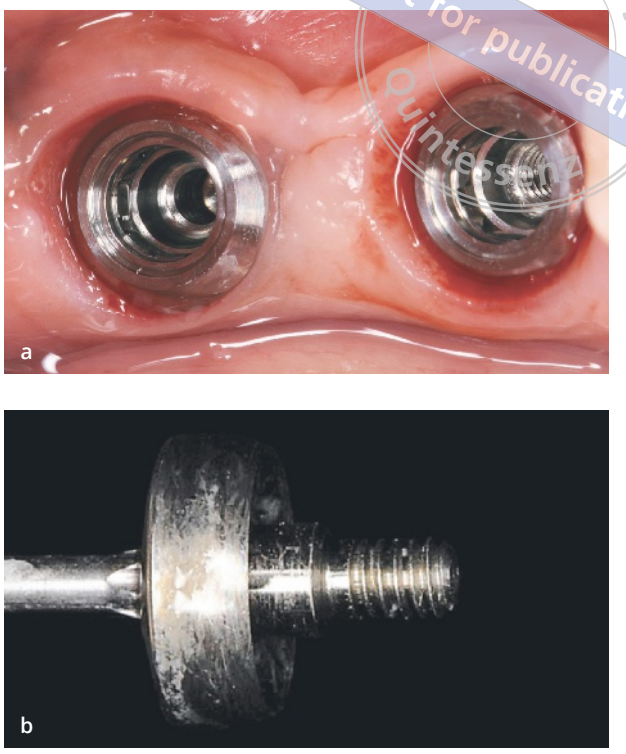

Figs 3-6a, b **(a)** Peri-implant mucositis can be established immediately after implant placement or uncovering if a single-phase or two-phase placement protocol is applied, respectively. In this case, inflammation was observed 6 weeks after implant placement. **(b)** Significant microbial deposits can be observed on the cover screw.

is more appropriate to include the following in the term peri-implant mucositis:

- Reversible inflammation that occurs in the peri-implant mucosa before functional loading that is due to the accumulation of the biofilm around the transmucosal healing screw (Figs 3-6a, b),[2,3] as well as reversible inflammation that occurs in the peri-implant mucosa after functional loading.

- **Peri-implantitis** represents a disease of the peri-implant tissues; it has a microbial etiology, which is accompanied by both inflammation of the peri-implant mucosa and destruction of the supporting bone of an implant. Peri-implantitis is directly related to the presence of biofilm but also to the patient's history of periodontitis and, if not treated effectively, may progress rapidly.[4]

Significant differences are observed between peri-implant mucositis and peri-implantitis, both clinically and histologically; in peri-implant mucositis, inflammation is limited to the soft peri-implant tissues (Figs 3-7a, b to 3-9a, b), whereas peri-implantitis causes irreversible damage to the supporting bone (Figs 3-10 to 3-12a–d).[5]

To detect even minor bone loss, it is necessary to keep a record of radiographic images of the implant at various stages, beginning immediately after placement, as illustrated in Chapter 7. Hence, it may be necessary to ascertain whether a radiographic image of a small amount of bone loss is due to bone remodeling, due to the connection of implant and transmucosal abutments, or if it is true bone loss due to peri-implantitis.[6] If peri-implantitis is untreated or poorly treated, it may progress rapidly (Figs 3-13a, b and 3-14a, b).[4]

As there is no defined peri-implant sulcus depth that indicates the transition from peri-implant mucositis to peri-implantitis, a record of the peri-implant sulcus depth measurements should be kept at various times, such as after prosthetic restoration and after the first year in function. It is important to note that probing depth ≥ 4 mm does not necessarily suggest the existence of a pocket.[7]

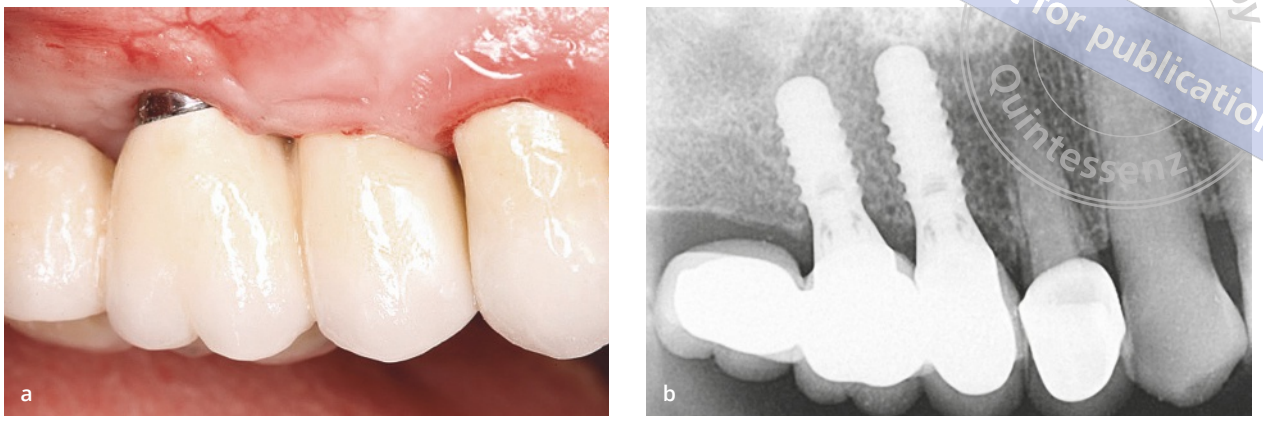

Figs 3-7a, b Clinical and radiographic images of peri-implant mucositis. Visible signs of inflammation, such as red, swollen, and bleeding soft tissues can be observed, while no bone loss is detected radiographically.

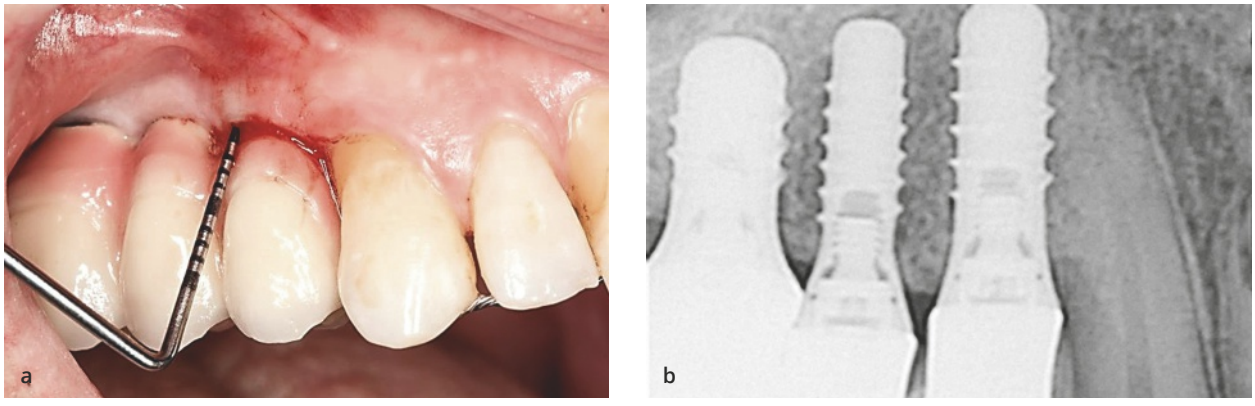

Figs 3-8a, b Clinical and radiographic images of peri-implant mucositis. BOP can be observed from the peri-implant sulci, while no bone loss is detected radiographically.

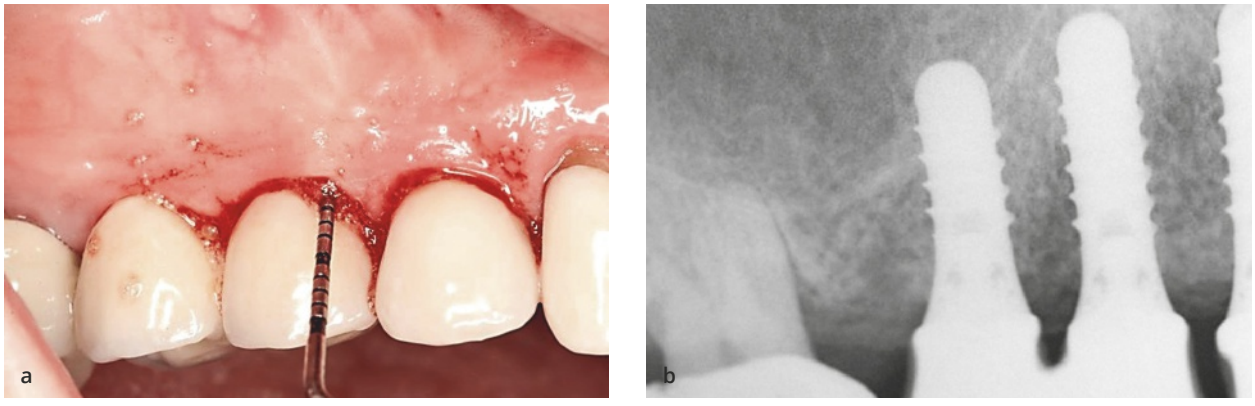

Figs 3-9a, b Clinical and radiographic images of peri-implant mucositis. Probing of peri-implant sulci leads to bleeding, while no bone loss is detected radiographically.

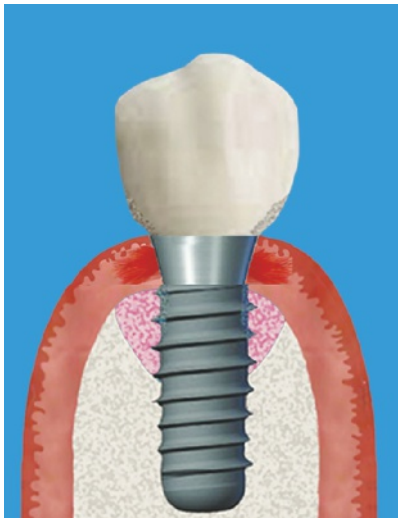

Fig 3-10 Schematic representation of peri-implantitis. Bone loss and exposure of the implant threads to the pocket environment can be observed. The microbial biofilm extends to the surface of the implant, over the exposed threads.

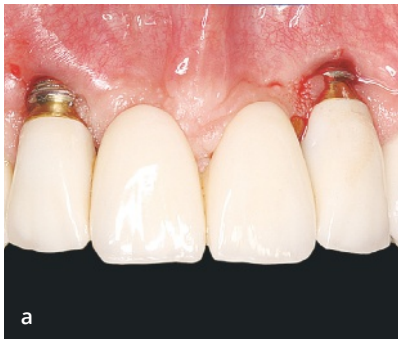

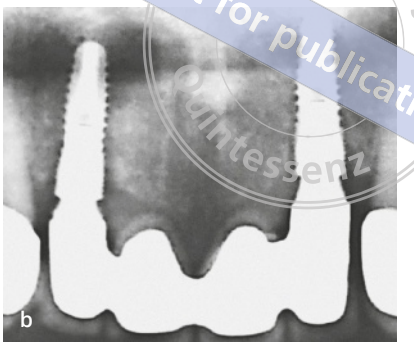

Figs 3-11a, b Clinical and radiographic images of peri-implantitis. There is a loss of soft peri-implant tissue attachment and BOP, while the radiograph reveals bone loss.

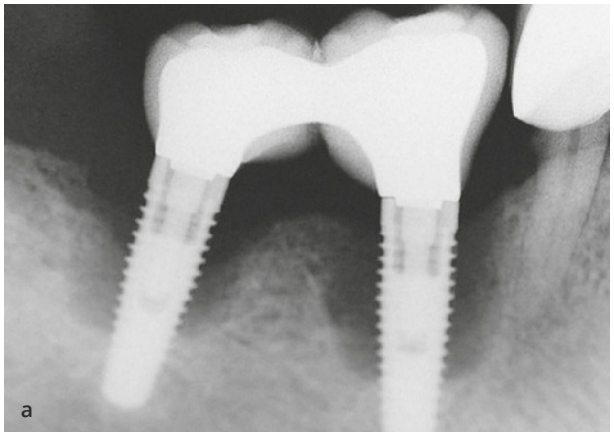

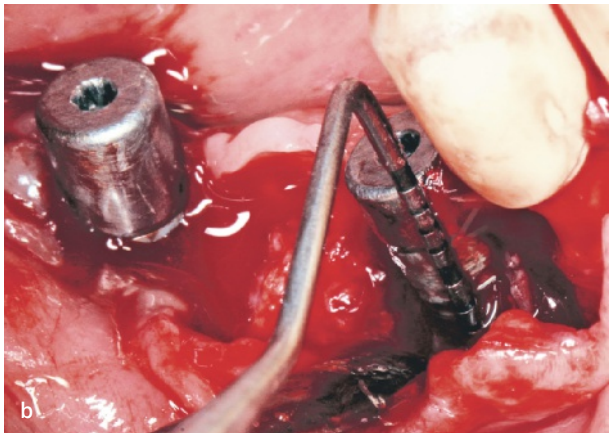

Figs 3-12a, b Radiographic and clinical images of peri-implantitis. Peri-implant bone loss in the fourth quadrant is evident in this patient who, for 10 years, remained without maintenance care. This is peri-implantitis due to biofilm accumulation.

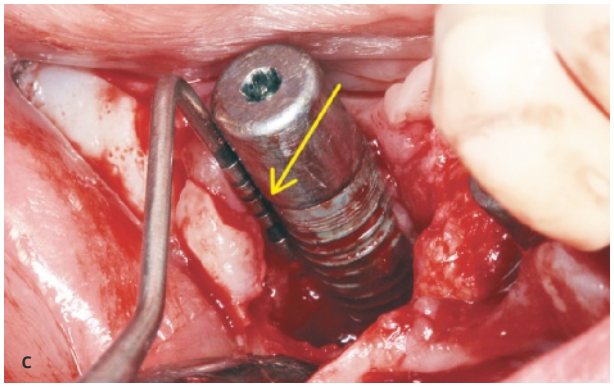

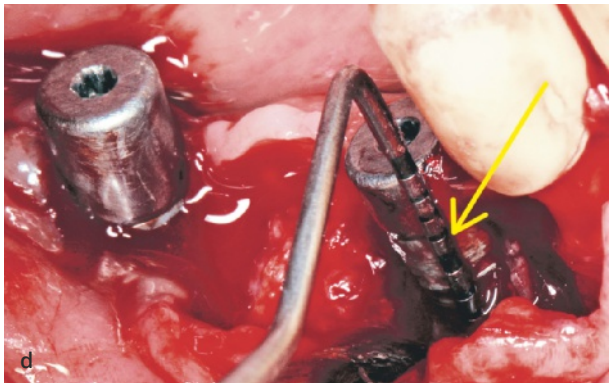

Figs 3-12c, d In addition to the extensive destruction of the peri-implant bone, the periodontal probe (yellow arrow) indicates 11 mm bone loss (for both implants) from the point of contact with the bone to the point of contact with the implant healing screw. The implants are 13 mm long. Therefore, the remaining bone support is only 2 mm.

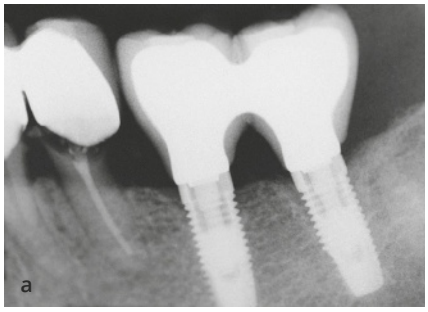

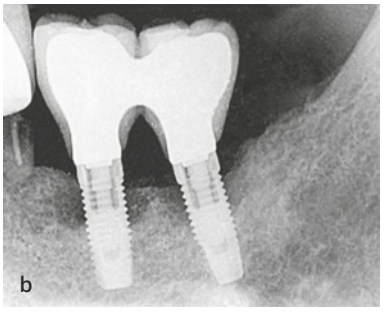

Figs 3-13a, b Radiographic image of implants **(a)** 7 and **(b)** 10 years after placement. Bone loss increased significantly, while caries destroyed tooth 35.

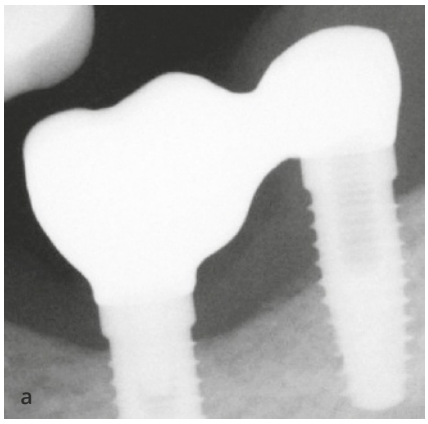

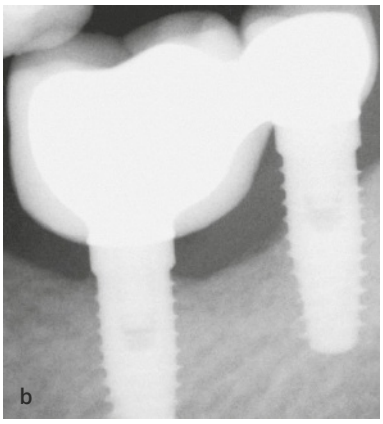

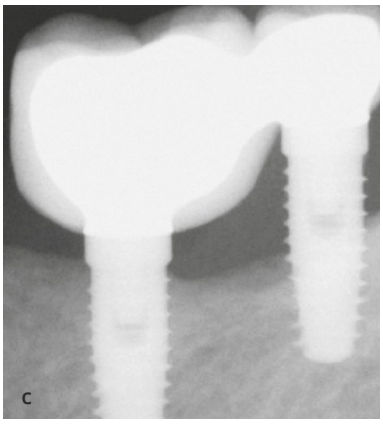

Figs 3-14a–c **(a)** Images of a patient's implants 6 years after placement. The implant in site 37 was placed incorrectly from the beginning and did not fully enter the alveolar bone. **(b)** The same area 1 year later, without having undergone any maintenance care. **(c)** Three years after implant placement, further bone loss is evident as peri-implantitis remained untreated. The case review continues in Chapter 10.

Peri-implantitis affects implants that have a prosthetic restoration and have undergone functional loading (Figs 3-15a–d and 3-16). It should not be confused with cases of early implant failure, where osseointegration is not achieved. In addition, during the first year after placement, a small amount of bone loss may be expected as part of the normal bone remodeling process. This is a radiographic finding but may not be accompanied by inflammation of the peri-implant mucosa.[8,9]

In this book, the term "iatrogenic peri-implantitis" is introduced to describe diseases caused by poorly designed or executed treatment. The most common case of iatrogenic peri-implantitis is that resulting from the presence of cement residue in the peri-implant sulcus. Because this is not a separate disease with different manifestations, signs, and symptoms, this topic is developed further in Chapter 5.

Some publications speak of "apical retrograde peri-implantitis". The term refers to the description of bone loss at the apical part of the implant due to the extension of peri-apical lesions from an adjacent tooth or from an incorrectly placed implant in an area with residual bone pathology of dental origin. These cases are rare, are managed with treatment of the primary lesion, and do not constitute a special category of peri-implantitis because they do not have a corresponding etiopathogenesis (Fig 3-17).[10–12]

Another category of peri-implant lesions includes cases of peri-implant bone loss and pocket formation due to periodontal pathology of an adjacent tooth. Periodontal pathology refers to cases of exacerbation of preexisting periodontitis or tooth fractures. In these cases, the term "secondary peri-implantitis" or "peri-implantitis due to an extension of inflammation from an adjacent tooth" may be used because the cause of peri-implant bone loss is inflammation and has a microbial etiology but the primary lesion is in an adjacent tooth and not on the implant surface (Figs 3-18a–n and 3-19).

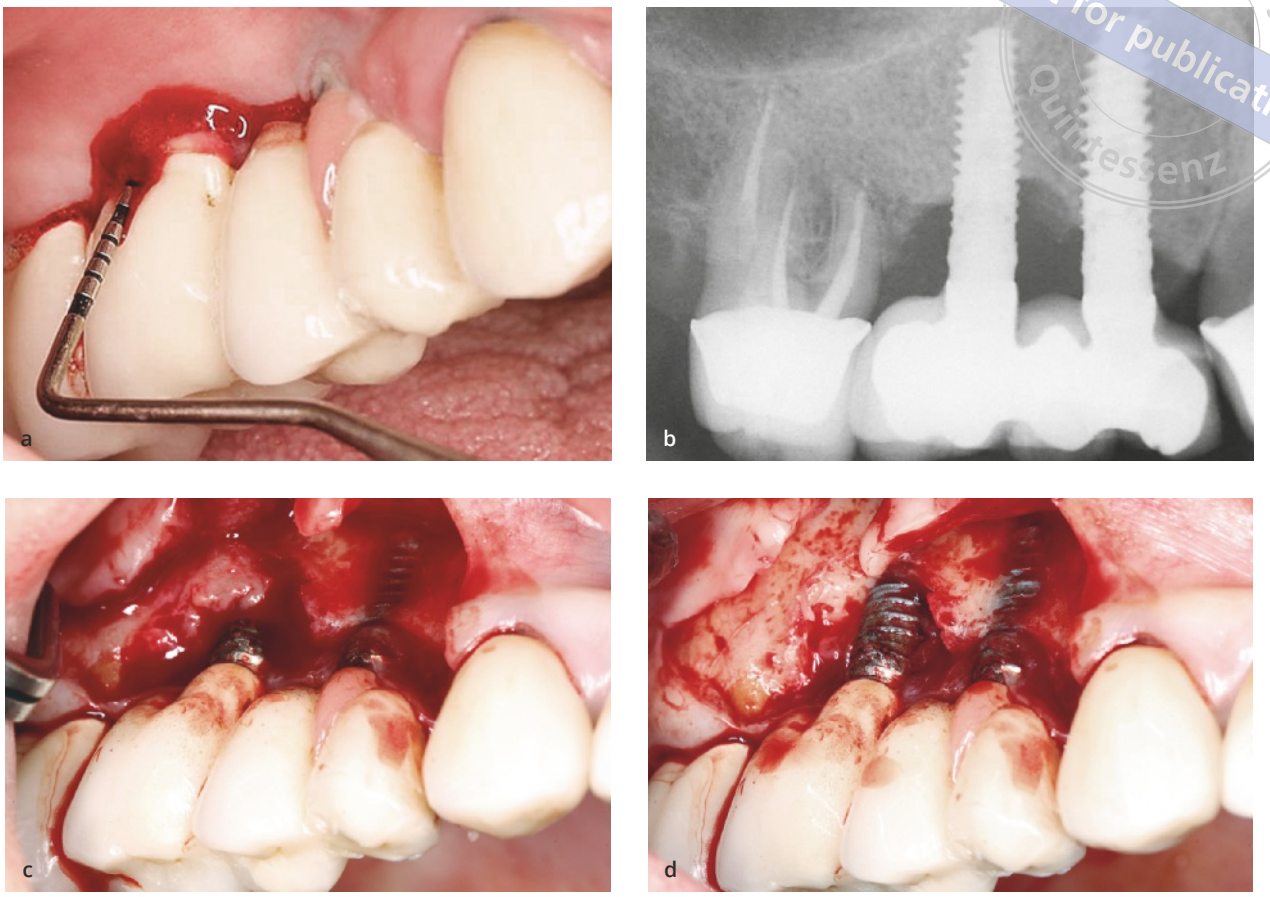

Figs 3-15a–d (a and b) Clinical and radiographic images of peri-implantitis. The deep expansion of the inflammation leads to bone loss and pocket formation while bleeding on probing is also detected. Radiographs give information about the size of the bone defect. **(c and d)** After the flap is elevated, the clinical inspection shows that the size of the defect was underestimated.

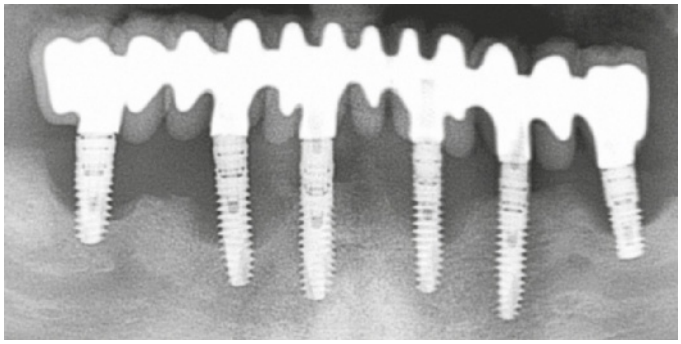

Fig 3-16 Radiograph showing peri-implantitis. Bone loss is extensive with characteristic saucer-shaped defects. Most implants now have little residual bone support.

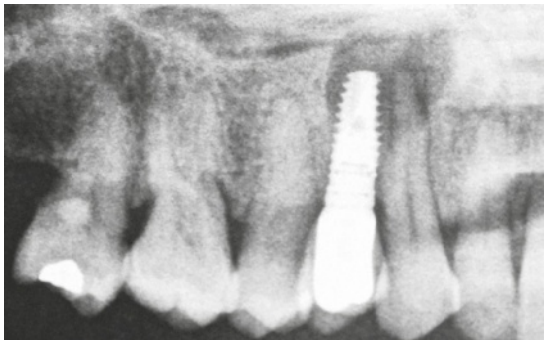

Fig 3-17 Radiograph of a patient with a lesion surrounding the apical part of implant 14 and tooth 13. This condition has also been described as "periapical peri-implantitis".

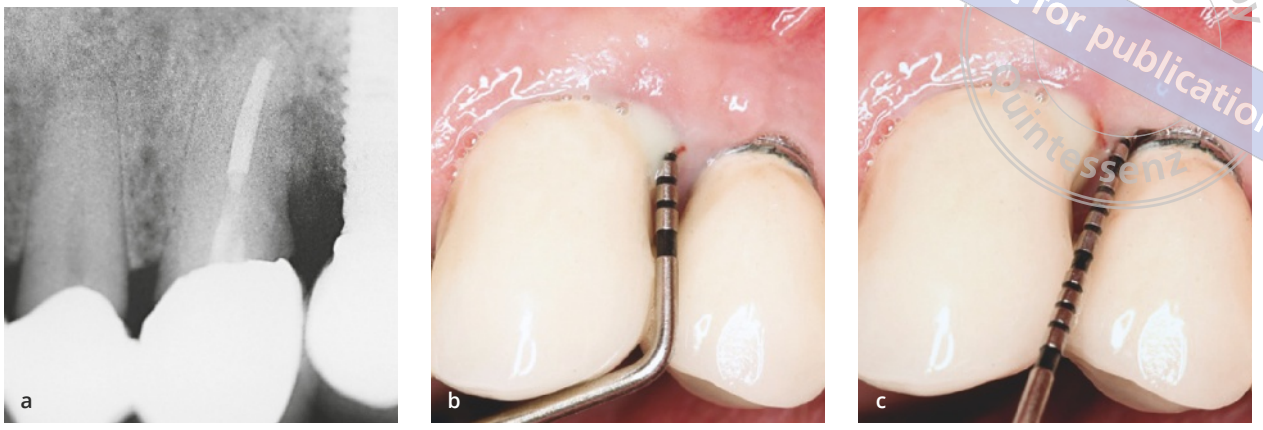

Figs 3-18a–c (a) Bone loss can be observed between tooth 23 and implant 24. **(b and c)** An 11-mm periodontal pocket is detected with suppuration from tooth 23 and the peri-implant sulcus at implant 24. Pus formation distal of tooth 23 is evident.

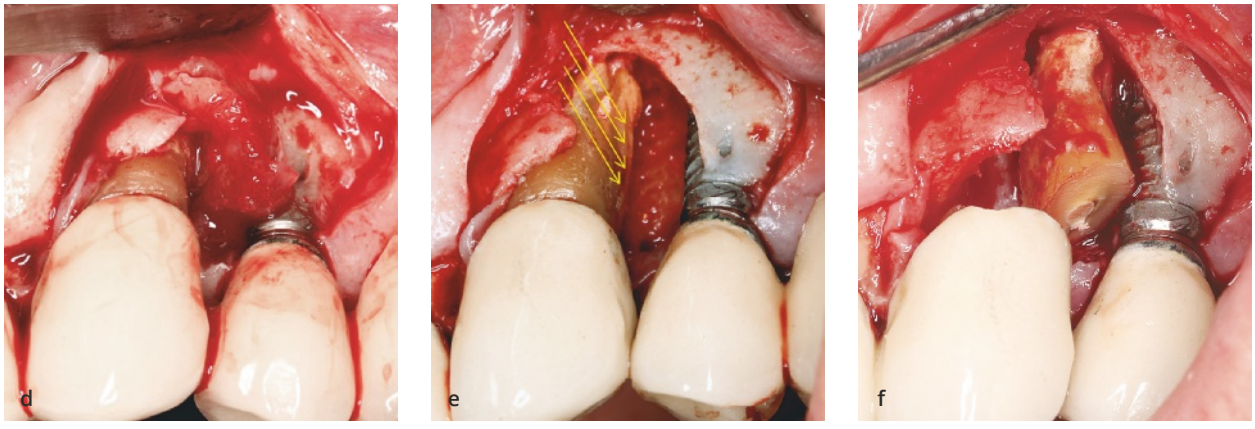

Figs 3-18d–f (d) After elevation of a diagnostic flap, a large amount of granulation tissue is found in the area where bone loss was shown radiographically. **(e)** After removal of the granulation tissue, a vertical fracture on the root of tooth 23 (yellow arrows) becomes visible, as well as extensive bone loss extending to the implant, leading to exposure of many threads. The palatal bone plate and the part of the buccal plate that is intact are visible. **(f)** The root of the tooth was amputated and carefully extracted so that the partial denture remained in situ.

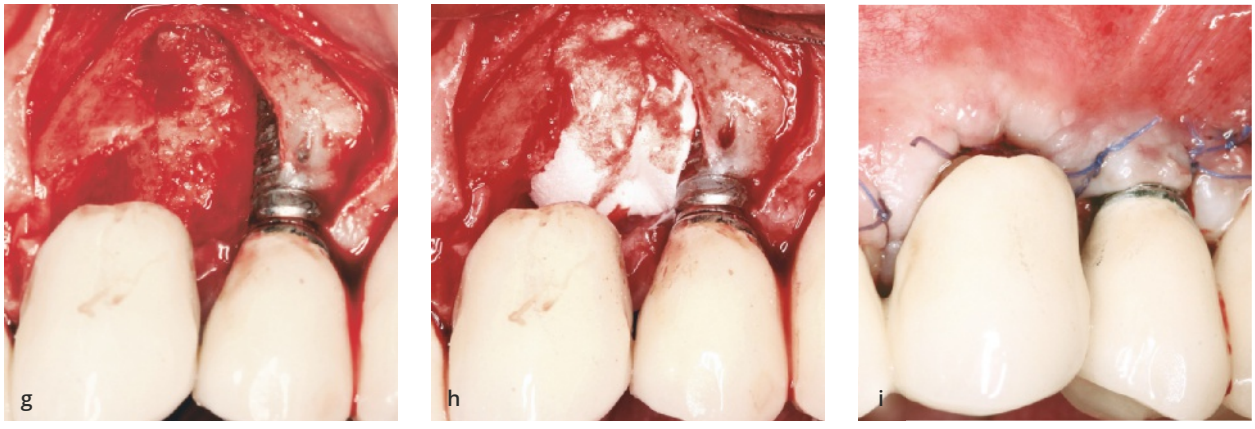

Figs 3-18 g–I (g) The root extraction area is visible. **(h)** Collagen graft placement. **(i)** Coronally repositioned flap and suturing.

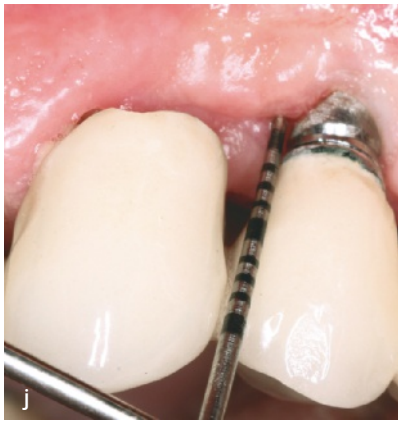

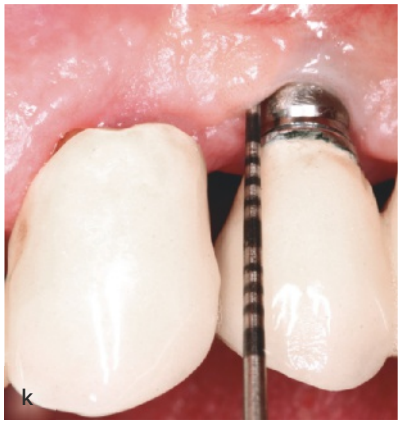

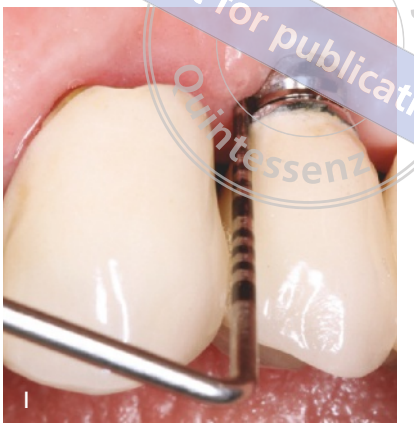

Figs 3-18j–l Peri-implant sulcus probing after **(j)** 3, **(k)** 6, and **(l)** 12 months shows peri-implant tissue stability.

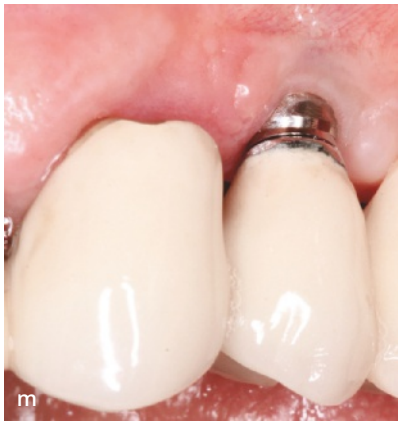

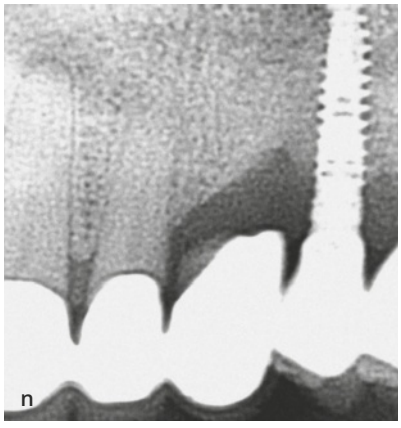

Figs 3-18m, n Clinical and radiographic images taken 2 years after surgery confirm that the peri-implant tissues are healthy and the bone–implant contact has been restored.

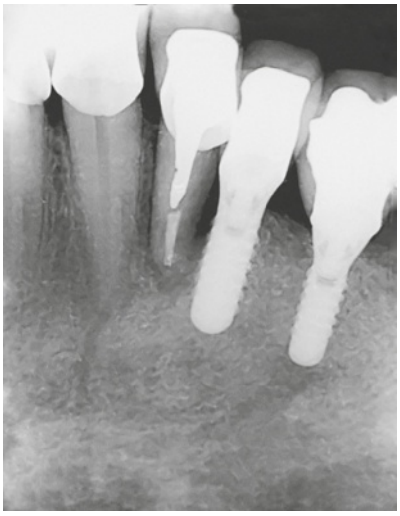

Fig 3-19 Radiographic image of secondary peri-implantitis. Bone loss is observed near the implant due to the pathology of tooth 34.

References

1. Heitz-Mayfield LJA, Salvi GE. Peri-implant mucositis. J Clin Periodontol 2018;45(suppl 20):S237–S245.
2. Pontoriero R, Tonelli MP, Carnevale G, Mombelli A, Nyman SR, Lang NP. Experimentally induced peri-implant mucositis. A clinical study in humans. Clin Oral Implants Res 1994;5:254–259.
3. Meyer S, Giannopoulou C, Cancela J, Courvoisier D, Müller F, Mombelli A. Experimental mucositis/gingivitis in persons aged 70 or over: microbiological findings and prediction of clinical outcome. Clin Oral Investig 2019;23:3855–3863.
4. Caton JG, Armitage G, Berglundh T, et al. A new classification scheme for periodontal and peri-implant diseases and conditions—Introduction and key changes from the 1999 classification. J Clin Periodontol 2018;45(suppl 20):S1–S8.
5. Renvert S, Persson GR, Pirih FQ, Camargo PM. Peri-implant health, peri-implant mucositis and peri-implantitis: case definitions and diagnostic considerations. J Clin Periodontol 2018;45(suppl 20):S278–S285.
6. Lindhe J, Meyle J. Peri-implant diseases: consensus report of the Sixth European Workshop on Periodontology. J Clin Periodontol 2008;35:282–285.
7. Lang NP, Bosshardt DD, Lulic M. Do mucositis lesions around implants differ from gingivitis lesions around teeth? J Clin Periodontol 2011;38:182–187.
8. Ericsson I, Lindhe J. Probing depth at implants and teeth. An experimental study in the dog. J Clin Periodontol 1993;20:623–627.
9. Berglundh T, Lindhe J, Ericsson L, Marinello CP, Liljenberg B, Thomsen P. The soft tissue barrier at implants and teeth. Clin Oral Implants Res 1991;2:81–90.
10. Singh R, Pandey V, Kumar V, Mishra AK. Retrograde peri-implantitis—A review of literature and an update. J Adv Med Dent Scie Res 2016;4:47–49.
11. Mohamed JB, Shivakumar B, Sudarsan S, Arun KV, Kumar TSS. Retrograde peri-implantitis. J Indian Soc Periodontol 2010;14:57–65.
12. Marshall G, Canullo L, Logan RM, Rossi-Fedele G. Histopathological and microbiological findings associated with retrograde peri-implantitis of extra-radicular endodontic origin: a systematic and critical review. Int J Oral Maxillofac Surg 2019;48:1475–1484.

Although much information exists on peri-implantitis, until now there has been a significant lack of concentrated knowledge and information on the subject presented in a book. This comprehensive publication solves that by summing up and assessing all the available information on peri-implant tissue pathology. It includes the authors' vast clinical experience and offers conclusions gained from the critical evaluation of scientific research. The text is accompanied by a plethora of images and schematic illustrations that support and help to interpret the scientific knowledge, while also offering a step-by-step methodology to complement the techniques presented.

The book is therefore an invaluable source of information and clinical guidance for clinicians and students regarding the prevention, diagnosis, and successful treatment of peri-implant diseases.

ISBN 978-1-78698-145-5

9 781786 981455

www.quintessence-publishing.com